

One Way or Another: Modes of Transport and International Trade

Edoardo Tolva *

ISEG Research and Universidade de Lisboa

January 2026

YOU CAN FIND THE LATEST VERSION [HERE](#)

Abstract

The transport sector is the backbone of international trade and has faced multiple disruptions in recent years. This paper studies how substitution across transport modes shapes international trade, welfare, and carbon emissions. Motivated by recent disruptions to air and maritime transport, I develop a quantitative multicountry trade model with multiple transport modes and endogenous congestion costs. I estimate the elasticity of substitution between transport modes at the country-pair level using the closure of Russian airspace as a quasi-natural experiment. I find an average elasticity of substitution between air and sea transport of 2.6. Counterfactual simulations show that allowing for mode substitution attenuates welfare losses from mode-specific transport shocks. However, since transport modes differ in carbon intensity, substitution also affects the environmental impact of trade and can weaken the effectiveness of environmental policies.

Keywords: Transport, Substitution, Ukraine, Suez, Trade costs, Carbon emissions

JEL Classification: F10, F12, F14, F18, R4, Q56

*Edoardo Tolva: ISEG Research, Universidade de Lisboa, Rua do Quelhas 6, 1200-781 Lisbon, email: edoardo.tolva@iseg.ulisboa.pt. I am very grateful to Dennis Novy and Marta Santamaria for their constant guidance and support in this project. I want to thank for the useful comments: Facundo Albornoz, Prottoy Akbar, Tibor Besedes, Natalie Chen, Paola Conconi, Davide Del Prete, Banu Demir, Alejandro Graziano, Anna Ignatenko, Pamina Koenig, Fabrizio Leone, Thierry Mayer, Gianmarco Ottaviano, Stephen Redding, Thomas Sampson, Bengt Söderlund, Carmen Villa, and Maurizio Zanardi. I also thank conferences and seminars participants at the Warwick Macro & International Workshop, CEP/Warwick Junior Trade Workshop, GEP-CEPR Annual Postgraduate Conference, RIEF, EAYE, European Urban Economic Association, SNEE, ETSG, Royal Economic Society Summer School, Journal of International Economics Summer School, Norwegian School of Economics, and Napoli Parthenope. All errors are my own.

1 Introduction

Transport plays a pivotal role in international trade, enabling the global movement of goods and sustaining both consumption and production across countries. At the same time, it is a major source of carbon emissions (Cristea et al., 2013; Shapiro, 2016). In recent years, the transport sector has been subject to unprecedented disruptions arising from both geopolitical events and natural phenomena. The Russian invasion of Ukraine in 2022 led to the closure of Russian airspace, severely disrupting air traffic between Europe and Asia, a corridor accounting for more than 20% of global air cargo volume (IATA, 2022). As air cargo has become increasingly important for international trade (Hummels, 2007; Feyrer, 2019), these restrictions carry potentially large economic consequences. Similarly, in 2023 and 2024 maritime trade was disrupted by events affecting the Panama Canal and the Red Sea, two critical chokepoints for global shipping.¹ At the same time, policy discussions aimed at reducing the carbon footprint of international transport have intensified, with potentially important implications for trade costs.

A common feature of these events is that they affect one transport mode at a time. The closure of Russian airspace primarily disrupted air routes, while attacks in the Red Sea targeted maritime transport. As a result, unaffected modes become relatively cheaper, creating incentives for substitution across transport modes that may partially offset the negative impact on trade flows. Because transport modes differ significantly in their carbon intensity, substitution also affects emissions from international trade. Yet, much of the international trade literature abstracts from this margin of adjustment by assuming that agents rely on a single transport mode. This assumption not only ignores heterogeneity across modes but also precludes substitution in response to mode-specific trade cost shocks.

Motivated by the central role of transport in global trade and the recent sequence of mode-specific disruptions, this paper studies how substitution across transport modes can act as a buffer against increases in transport costs. In addition, I analyze how this substitution margin shapes the environmental consequences of international trade.

I address these questions using both empirical and theoretical approaches. First, I document the widespread use of multiple transport modes within narrowly defined product categories and origin–destination pairs. Second, I develop a quantitative Ricardian model of trade that incorporates multiple transport modes and endogenous transport costs. Third, I exploit an exogenous trade cost shock to provide novel estimates of the elasticity of substitution between transport modes. Finally, I use the model to evaluate a set of counterfactual scenarios in which a specific transport mode is disrupted, quantifying the implications for welfare. I also show that substitution across modes can substantially affect the effectiveness of environmental policies targeting the transportation sector.

While maritime transport continues to dominate global trade by volume, air cargo has grown steadily in both volume and value (Hummels, 2007; Feyrer, 2019; IATA, 2025). Using Eurostat data, I show that air transport accounts for approximately 30% of extra-European trade value

¹ Around 30,000 ships per year transit these two waterways, accounting for more than 20% of global seaborne trade. Source: [Unctad \(2024\)](#).

and that more than 70% of origin–destination–sector triplets use both air and sea transport. This evidence indicates that agents engaged in long-distance trade typically have access to multiple transport modes and can therefore adjust their mode choice when one becomes more costly.

Motivated by these facts, I extend a standard Ricardian model of trade ([Eaton and Kortum, 2002](#); [Dekle et al., 2007](#)) to allow for multiple transport modes in international shipping. The choice of transport mode is modeled as a discrete decision made after import quantities are determined for a given origin. Importers select the mode based on transport prices and idiosyncratic preferences for shipments between two locations. This structure delivers two key equilibrium objects: the mode-specific trade shares and a transport cost price index. The latter can be interpreted as an iceberg trade cost that, together with country-specific price distributions, determines aggregate trade flows. A central parameter of the model is the elasticity of substitution between transport modes, which governs the extent to which agents can reallocate shipments across modes. A key advantage of this framework is that it nests within the “universal gravity” structure ([Allen et al., 2020](#)), allowing standard quantitative trade models to be extended in a tractable way to incorporate multiple transport modes.

Allowing for substitution across transport modes introduces a novel margin of adjustment relative to the standard trade literature. This margin has two main implications. First, welfare losses from increases in transport costs are mitigated as agents partially switch to alternative modes. Second, the change in the transport cost index varies across country pairs depending on their exposure to the disrupted mode, generating asymmetric effects that cannot be replicated by models with a single iceberg trade cost.

The model also features congestion forces that limit substitution. As demand for a given transport mode rises, its price increases, making bilateral transport costs endogenous to usage. Consequently, a mode-specific cost shock triggers two opposing forces. On the one hand, substitution toward the unaffected mode raises its price through congestion. On the other hand, higher transport costs reduce bilateral trade volumes, which alleviates congestion and partially offsets the initial shock. By solving the model in changes, I show that the only additional data requirement relative to a standard Ricardian model is information on initial trade shares by mode for each country pair.

I estimate the elasticity of substitution between transport modes using the Ukraine–Russia conflict as an exogenous shock to transport costs. Sanctions imposed between the European Union and Russia led to the closure of Russian airspace, significantly increasing air transport costs ([IATA, 2022](#); [Chu et al., 2024](#)). I implement a difference-in-differences (DiD) strategy that compares changes in flight times and trade shares by mode between affected and unaffected country pairs before and after the outbreak of the war. To this end, I combine flight-level data from nearly two million flights recorded by OpenSky with Eurostat data on trade flows. I first show that the conflict substantially increased flight times between Europe and East Asia, and then document a corresponding shift toward maritime transport in affected routes. Dividing the estimated effect on mode shares by the effect on transport times yields a Wald-DiD estimate of the elasticity of substitution between modes ([Wald, 1940](#); [Angrist and Pischke, 2009](#);

[De Chaisemartin and d'Haultfoeuille, 2023](#)). I estimate this elasticity to be approximately 2.6. I also document substantial heterogeneity across products: goods that are non-perishable and have a high value-to-weight ratio, such as textiles, exhibit the highest substitutability across modes.

As an alternative identification strategy, I exploit the 2021 disruption at U.S. West Coast ports ([Hu et al., 2021](#)). A key advantage of this setting is that I directly observe transport charges paid by importers. Using a similar DiD design, I define treated countries as U.S. trading partners in Asia and use European countries as a control group. Both empirical strategies yield statistically similar estimates of the elasticity of substitution between transport modes. Given the prolonged nature of these disruptions, I interpret the estimated elasticities as reflecting medium- to long-run adjustments.

In addition to the substitution elasticity, the model features a congestion parameter governing how transport prices respond to usage. I estimate this parameter using a shift-share instrumental variables approach ([Borusyak et al., 2022, 2025](#)). Using U.S. Census data on imports,² I construct instruments based on variation in imports across origins within narrowly defined sectors. As a robustness check, I also use European exports to non-U.S. destinations as an alternative shifter. I estimate the congestion parameter to be approximately 0.06 for maritime transport, consistent with existing estimates such as [Fuchs and Wong \(2024\)](#), and around 0.10 for air transport. To my knowledge, this paper provides the first estimate of congestion effects in air cargo transport.

I calibrate the model using trade flow data from Comtrade and mode-specific trade shares assembled from the U.S. Census Bureau, Eurostat, the Japan Customs Authority, the Inter-American Development Bank, and the ASEAN Secretariat. The resulting dataset covers trade by mode for 33 countries, with Europe treated as a single bloc and two transport modes: air and sea. I use the calibrated model to simulate the effects of transport disruptions on trade flows, welfare, and CO₂ emissions.

I conduct three counterfactual exercises: the closure of Russian airspace, the closure of the Suez Canal, and a policy targeting carbon emissions in maritime transport. I compare a baseline model with endogenous mode substitution to a model with fixed Cobb–Douglas shares across modes. In all cases, allowing for substitution reduces welfare losses, as agents partially reallocate shipments toward unaffected modes. For example, in the Suez Canal experiment, average welfare losses are 0.05 percentage points smaller, an improvement of about 6.2%, when substitution is allowed. While these aggregate effects may appear modest, even small welfare changes can have substantial economic significance at the level of entire economies.

Substitution across transport modes also has important implications for environmental policy. Because air and sea transport differ substantially in carbon intensity, substitution can undermine policies that target emissions in a single mode. I show that a policy aimed at reducing emissions from maritime transport achieves a reduction in total transport-related emissions that

²Eurostat does not report transport costs, which prevents estimating congestion effects using European data.

is almost 20% smaller once substitution toward air transport is taken into account.³

From a policy perspective, the results highlight the importance of accounting for transport mode substitution when designing trade and environmental policies. Mode-specific disruptions, whether caused by geopolitical events, infrastructure bottlenecks, or climate-related shocks or regulations, do not translate one-for-one into trade cost increases once agents can reoptimize their transport choices. Ignoring this adjustment margin can lead to systematic overestimation of welfare losses from transport shocks and mismeasurement of their distribution across countries. At the same time, substitution across modes can substantially weaken the effectiveness of environmental policies that target emissions in a single segment of the transport sector, as reductions in one mode may be partially offset by shifts toward more carbon-intensive alternatives. These findings suggest that policies aimed at improving the resilience and sustainability of international trade, such as infrastructure investments, carbon pricing, or mode-specific regulations, should be evaluated in a framework that jointly considers multiple transport modes, congestion effects, and endogenous substitution.

Related Literature. This paper contributes to the literature studying the relationship between international trade and transport modes. Existing work typically frames this relationship as a trade-off between speed and cost, emphasizing the value of timely delivery in hedging against uncertainty or responding to demand shocks. The choice of transport mode has been shown to depend on the quality and characteristics of shipped goods (Hummels and Skiba, 2004; Hummels, 2007; Hummels and Schaur, 2013), delivery timing and reliability (Evans and Harrigan, 2005; Hummels and Schaur, 2010), and relative prices across modes (Micco and Serebrisky, 2006; Harrigan, 2010). Technological progress has played a central role in the long-run expansion of air transport in international trade (Campante and Yanagizawa-Drott, 2018; Feyrer, 2019). Even when studying transport disruptions, however, the literature has largely focused on the direct effects on the affected mode, abstracting from the possibility that firms adjust by switching to alternative modes (Carballo et al., 2014; Söderlund, 2020; Coşar and Thomas, 2021; Feyrer, 2021; Sandkamp et al., 2022; Al-Malk et al., 2024; Besedeš et al., 2024; Ludwig, 2025).

From an empirical perspective, this paper provides novel estimates of the elasticity of substitution between transport modes at the country-pair level. To my knowledge, this is the first study to identify this elasticity using quasi-natural experiments that generate plausibly exogenous variation in relative transport costs. Hummels and Schaur (2013) provides early evidence of substitution across modes and reports elasticities of comparable magnitude, though in a different empirical setting. More recently, Fuchs and Wong (2024) estimates a related parameter for land transport, while Ko et al. (2025) recovers sectoral trade elasticities by mode exploiting geographic variation across country pairs.⁴

³This experiment is inspired by the International Maritime Organization (IMO) policy framework, which—effective from 2023—aims to reduce shipping emissions by 40% by 2030 and 70% by 2050 relative to 2008 levels (Lugovskyy et al., 2023).

⁴An earlier unpublished working paper by Lux (2011) also examines substitution across transport modes in

From a theoretical perspective, the paper augments standard multicountry Ricardian models of trade (Eaton and Kortum, 2002; Allen et al., 2020) by allowing for multiple transport modes, thereby enabling the analysis of mode-specific trade cost shocks and their aggregate welfare consequences. In doing so, it contributes to the growing literature on endogenous transportation costs in international trade and spatial economics (Allen and Arkolakis, 2014; Asturias, 2020; Brancaccio et al., 2020; Fajgelbaum and Schaal, 2020; Wong, 2022; Jaworski et al., 2023; Fuchs and Wong, 2024; Do et al., 2024). This paper is the first to combine substitution across transport modes with endogenous transportation costs driven by congestion and demand in a tractable multicountry general equilibrium framework. In addition, I provide the first estimates of the congestion elasticity for air transport, using a shift-share identification strategy (Borusyak et al., 2022, 2025), and show that its magnitude is comparable to estimates for other transport modes (Fuchs and Wong, 2024).

Finally, the paper contributes to the literature on the environmental impacts of international trade (Cristea et al., 2013; Shapiro, 2016, 2021; Mundaca et al., 2021; Copeland et al., 2022; Lugovskyy et al., 2023; Hansen-Lewis and Marcus, 2022; Felbermayr et al., 2023; Sogalla et al., 2024; Ludwig, 2025) by introducing substitution across transport modes as an additional adjustment margin. While existing studies typically assume fixed trade shares by mode, the framework developed here allows firms to reallocate shipments across modes in response to policy-induced changes in transport costs. This mechanism has first-order implications for the effectiveness of environmental policies targeting emissions in the transport sector, as reductions in one mode may be partially offset by substitution toward more carbon-intensive alternatives.

2 Data and Facts

In this section, I introduce the main dataset used for my empirical analysis and then present some key statistics on trade by transport mode that will motivate the structure of the model.

2.1 Eurostat Data

I use monthly data from Eurostat on European imports and exports by transport mode between countries. Flows are reported both in terms of value (in euros) and weight (kg).⁵ There are four main modes of transport: air, rail, road, and sea, which collectively account for approximately 95% of total trade in the sample.⁶ The data are provided at the 6-digit product code level following the Harmonized System (HS) classification, which allows for a detailed study of how goods are transported. The data cover the period from January 2010 to December 2022.

international trade. That study differs substantially from this paper. Empirically, it relies on descriptive correlations rather than quasi-exogenous variation. Theoretically, it does not provide a structural framework linking observed mode shares to a well-defined elasticity of substitution.

⁵All transactions with a weight below 100 kg are reported as zero in Eurostat.

⁶I discard the remaining modes, including unknown, post, fixed mechanisms, inland waterways, and self-propulsion, either because they are seldom used or because I cannot categorize them, such as post or non-categorized.

I focus on trade flows reported as air and sea, accounting for approximately 80% of the total value, to avoid measurement errors in land transport. A limitation of this dataset is that, for a few country pairs, some modes are reported as being used even if it is geographically impossible. For instance, flows from the US to Germany via road or rail are reported as greater than zero for some sectors. This discrepancy arises because some customs declarations are processed when they enter the Eurozone.⁷

Finally, to minimize the number of zeros, I exclude small countries, restricting my sample to the 80 largest nations in terms of GDP (World Bank data, 2019), which account for approximately 93% of total trade. I also exclude the United Kingdom as it dropped from the sample of reporting countries after 2020, as well as Russia and Ukraine because of the ongoing conflict.

This dataset has two main limitations. First, It does not report transport costs by mode. Second, it contains data on trade flows only with extra-European countries.⁸ Although intra-EU flows are available from 2010 onward on Eurostat, they are reported at a higher level of aggregation using the Standard Goods Classification for Transport Statistics (NST), which is divided into 20 sectors and collected via survey rather than customs declarations. Additionally, most intra-EU trade is conducted via road ([Santamaría et al., 2023](#)). The predominant use of road transport is due to the relatively short distances within Europe compared to international routes. As a result, air transport is seldom used, and the geography of the continent does not favor trade via large ships.

2.2 US Census Bureau Data

As an alternative data source, I also collect data from the US Census Bureau.⁹ This allows me to obtain data on US trade by mode of transport at a monthly frequency via their API. Similar to the Eurostat data, trade flows are reported at the 6-digit HS level. The data are available from January 2013 to December 2022. In this case, only US import flows by air and sea are reported. This is due to the geography of the US which borders via land only with Canada and Mexico. The key difference is that this dataset contains the total freight cost incurred along the origin-sector-mode to transport the goods to the us.

2.3 Composition of European Imports and Exports by Transport Mode

In this section, I document two key facts about trade and transport modes. First, European countries rely heavily on multiple modes of transport for their imports and exports outside the European Union. Second, even within the same origin-destination-product triplet, we often observe multiple modes at the same time. These two facts taken together will motivate augmenting a Ricardian model of trade with multiple modes of transport.

⁷For example, if a shipment by plane from the US lands in Switzerland and is then transported to Germany by truck without passing through Swiss customs, it will be reported as a German import from the US via truck. Reporting problems are common in international trade datasets ([Cotterlaz and Vicard, 2023](#)).

⁸For example, Germany-China is included, but Germany-France is not.

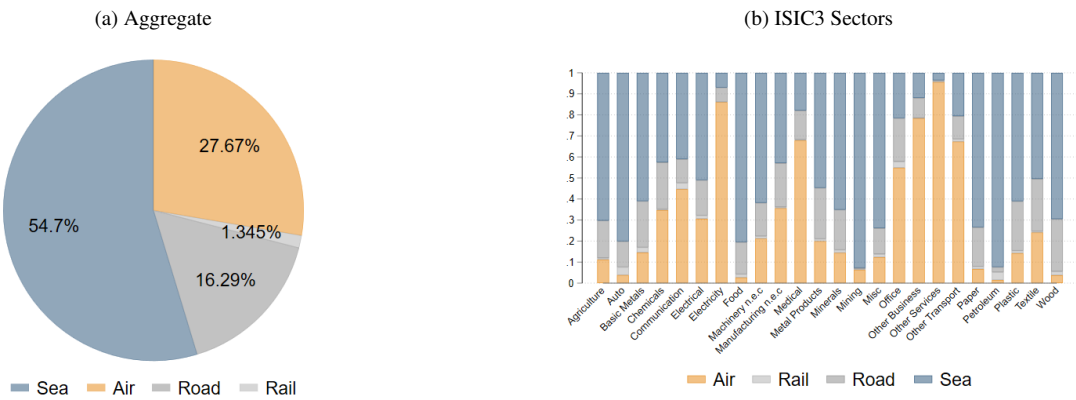
⁹see for example, [Hummels \(2007\)](#); [Hummels and Schaur \(2010, 2013\)](#).

Fact I: Relevance of Multiple Modes of Transport. The total value of trade transported via air is approximately 760 billion euros, accounting for around 28% of the total trade value. This can be seen in figure 1a, which reports the composition of aggregate European trade with non-European countries by mode in 2019, measured in euros. This means that a significant portion of trade is conducted via air transport, despite its higher cost. Figure D.1 shows that the patterns are almost identical when considering imports and exports separately. In Figures D.2, we can see that air and sea transport account for almost all trade with China and the United States, which are among Europe's main partners.

While there is dispersion across different sectors, the use of air transport is widespread, as we can see in figure 1b where products are divided based on their HS Section. Air transport is predominantly used for high value, low-weight goods such as electronics, pharmaceuticals, and precision machinery, which exhibit high value-to-weight ratios. In contrast, sea transport is the preferred mode for heavy, lower-value goods, including raw materials and petroleum products (Hummels, 2007).

Since air and sea are clearly the predominant modes of transport for international trade in I will focus on these two modes from here onward.

Figure 1: Transport Mode Share of Trade

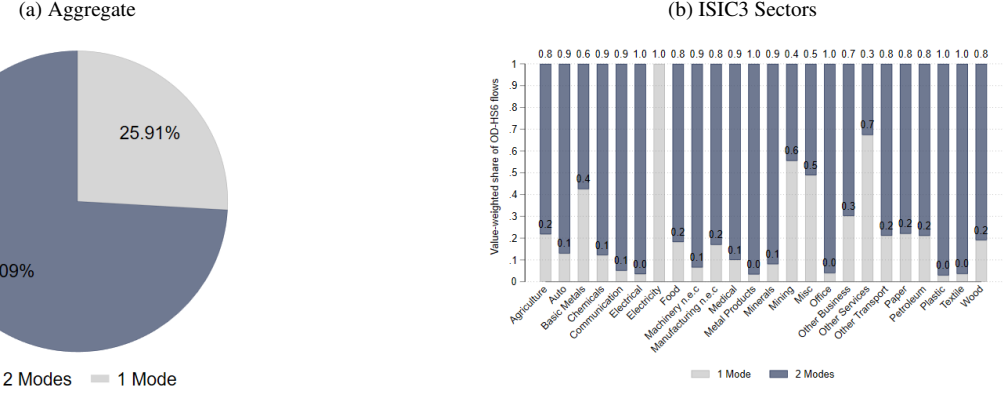


Notes: Panel (a) reports the aggregate share of trade in euros by mode of transport. Panel (b) reports the same statistics by HS section. The sample consists of imports and exports of European Union members in 2019, collected from Eurostat.

Fact II: Multiple Modes in the Same Origin-Destination-Product. A vast majority of the origin-destination-sector triplets use two modes of transport at the same time to conduct trade. This can be seen in figure 2 where I show that around 74% of origin-destination-sector triplets utilize two modes of transport. As before, a sector is defined as an HS6 product category, providing a very fine product level definition.¹⁰ As before, the same phenomenon can be observed if we examine imports and exports separately, figure D.4, or even more strongly when we analyze trade with the US and China, Figure D.5.

¹⁰This pattern is robust even if we look at unweighted data or data weighted by kilos instead of value, as shown in Figure D.3.

Figure 2: Number of Modes Used per Origin-Destination-HS6



Notes: Panel (a) shows the percentage of origin-destination-HS6 sectors that use both air and ocean transport. Panel (b) shows the same distribution across ISIC3 sectors. The sample consists of imports and exports of European Union members in 2019, collected from Eurostat.

Product' characteristics do matter in defining which products can be shipped, but I still find that this pattern holds across broadly defined sectors, as shown in panel (b) of Figure 2.

Taken together, these two facts indicate that the use of multiple modes of transport is a salient feature of international trade. The Data from the US Census Bureau show very similar patterns in terms of value and weight traded by transport mode. Appendix A.1 provides more information on the US data and a comparison with the European data. This is in line with other studies that have shown similar features, using even more detailed data for the US ([Hummels and Schaur, 2013](#)). Therefore, models that assume a single mode of transport fail to capture these patterns, which I address in the next section by incorporating them into a simple Ricardian framework.

3 Model

In this section, I combine a discrete choice model with a Ricardian trade framework. The model builds on the standard multi-country trade model of [Eaton and Kortum \(2002\)](#), which determines global trade flows, wages, and prices. The discrete choice model over transport modes endogenously determines the equilibrium modal shares in bilateral trade and delivers a transport price index, which enters the trade model as an iceberg trade cost. In addition, the model features congestion costs at the origin–destination–mode level that affect transportation prices along each route. To highlight the key mechanism, I focus on a single-sector economy, though the framework can be extended to multiple sectors in a tractable way.

3.1 Setup

Consider an economy with countries indexed by $n = 1, \dots, N$. Each country is endowed with L_n units of labor, which are supplied inelastically and allocated between manufacturing and non-manufacturing sectors. I assume that workers can move freely across sectors, but migration across countries is not allowed. Furthermore, I assume a continuum of goods $u \in [0, 1]$ and

perfect competition in each market. Consumers in country n maximize the following constant elasticity of substitution (CES) utility function:

$$U_n = \left(\int_0^1 Q_n(u)^{(\sigma-1)/\sigma} du \right)^{\sigma/(\sigma-1)}. \quad (1)$$

Production combines labor and intermediate inputs, with labor accounting for a constant expenditure share β . Moreover, I assume the presence of a non-tradable sector, which is combined with manufacturing output to produce the final consumption good through a Cobb-Douglas aggregator. The share of total expenditure for the tradable good is α . Similarly to [Dekle et al. \(2007\)](#), I define the exogenous deficit in manufacturing as the difference between production and imports: $D_n^{Ma} = X_n^{Ma} - Y_n^{Ma}$, while the overall exogenous trade deficit is defined as $D_n = X_n - Y_n$.

3.2 Multiple Modes of Transport

The first departure from a standard Ricardian trade model is that I allow for $m = 1, \dots, M$ distinct modes of transport. This assumption is motivated by the widespread use of multiple modes within the same origin–destination–product pair, as documented in Section 2. Let d_{ni}^m denote the iceberg trade cost of shipping goods from origin $i \in N$ to destination $n \in N$ using mode $m \in M$.¹¹

3.2.1 Main Assumption

I make a series of assumptions to model the choice of transport mode. First, I assume a two-step decision process for consumers in each country. Buyers first choose the source country from which to purchase goods and then select the mode of transport. In the first step, consumers compare factory-gate prices adjusted by transport cost indices across all origins. Conditional on the chosen origin, they then select the transport mode.

A second assumption throughout the paper is that factory-gate prices are independent of the transport mode. Specifically, producers set prices solely as a function of their productivity, while transport costs, which are borne by the importer, do not affect this pricing decision.¹² Another key assumption is the simultaneous availability of all transport modes without capacity or infrastructure constraints.¹³ This framework permits the use of a discrete choice model in which the share of each transport mode is strictly positive. While this assumption may appear strong, empirical evidence shows that many goods are shipped using both air and sea transport, as illustrated in Figure 2.

¹¹Mode-specific trade costs for the same origin–destination–product pair are common in the data ([Hummels, 2007](#)). For example, air transport is faster than sea shipping but entails higher per-unit costs.

¹²This assumption is standard in trade models and allows trade costs to be expressed as a fraction of the good’s value. Here, I extend this logic to mode-specific transport costs.

¹³This is a common assumption in trade models that abstract from capacity constraints. [Rich et al. \(2011\)](#) note that structural rigidities can limit the substitutability across transport modes.

The transport sector is assumed to operate under perfect competition. Market power in transportation would introduce additional trade frictions (Humelis et al., 2009; Asturias, 2020; Ignatenko, 2020; Cristoforoni et al., 2025). I exclude this additional channel to focus more directly on the impact of substitution across modes.

3.2.2 Discrete Choice Model of Transport Modes

Given the assumptions in the previous section, I can model the choice of transport mode as a discrete choice problem. In each country n , there is a continuum of importers. Conditional on choosing origin i from which to purchase goods, importers choose among M transport modes. I follow Anderson et al. (1987) and show that a CES demand system for transport can be derived from a nested logit model with a deterministic second stage

In Appendix C.1, I solve the discrete choice problem and show that the price index faced by importers in country n when importing goods from origin i is given by:

$$p_{ni} = \left(\sum_{m=1}^M (p_{ni}^m)^{1-\eta} \right)^{1/(1-\eta)} = p_i \left(\sum_{m=1}^M (d_{ni}^m)^{1-\eta} \right)^{1/(1-\eta)} = p_i d_{ni}, \quad (2)$$

where the last equality follows from substituting the definition of the mode-specific price and using the fact that the CES price index is homogeneous of degree one.¹⁴ Equation (2) makes clear that d_{ni} plays the role of the standard iceberg trade cost used in the literature. I therefore define

$$d_{ni} = \left(\sum_{m=1}^M (d_{ni}^m)^{1-\eta} \right)^{1/(1-\eta)}, \quad (3)$$

as the transport cost index paid when importing goods into country n from origin i .

This is the analog of the standard iceberg trade cost used in quantitative trade models. The difference is that, in my framework, it is derived by aggregating mode-specific costs. I can therefore use d_{ni} as the relevant trade cost that importers consider when choosing where to source goods from. This allows me to rely on well-established results from the literature while introducing an additional margin of adjustment. As noted above, I abstract from other bilateral trade costs such as tariffs, τ_{ni} . If tariffs are included, the price index in (2) becomes $p_{ni} = p_i \tau_{ni} d_{ni}$.¹⁵

Finally, this demand system implies that the share of trade by mode between two countries is given by:

$$\pi_{ni}^m = \frac{(d_{ni}^m)^{1-\eta}}{\sum_k (d_{ni}^k)^{1-\eta}} = \frac{X_{ni}^m}{X_{ni}}, \quad (4)$$

where X_{ni}^m is the value imported by n from i by mode m , X_{ni} is the total value imported, and η represents the elasticity of substitution between transport modes within country pairs. Given

¹⁴This is where the assumption that factory-gate prices are independent of the transport mode is crucial, since it implies $p_i^m = p_i ; \forall m \in M$.

¹⁵For the rest of the paper, I assume $\tau_{ni} = 1$. Since I solve the model in changes, constant terms drop out, so assuming fixed tariffs or no tariffs is equivalent.

the assumptions of the CES demand system, we have the restriction that $\eta > 1$.

3.2.3 Elasticity of Substitution

Starting from equation (4), the share of trade by mode between a pair of countries depends on relative mode-specific trade costs and the parameter η , which governs the elasticity of substitution across transport modes. In the next section, I use an exogenous shock to transport costs to estimate the parameter η .

In particular, I exploit relative variation in transport costs by mode. To see this, take logs of (4):

$$\ln \left(\frac{X_{ni}^m}{X_{ni}} \right) = (1 - \eta) \ln \left(\frac{d_{ni}^m}{d_{ni}} \right),$$

Next, taking ratios between two generic modes m and s yields

$$\ln \left(\frac{X_{ni}^m}{X_{ni}^s} \right) = (1 - \eta) \ln \left(\frac{d_{ni}^m}{d_{ni}^s} \right). \quad (5)$$

Thus, the coefficient $(1 - \eta)$ captures the elasticity of the modal trade share with respect to changes in relative transport costs across modes.

3.3 Congestion

I assume the presence of mode-specific transport costs, d_{ni}^m , between countries i and n . I further assume that these costs depend on a fundamental component, δ_{ni}^m , and a congestion component, Ξ_{ni}^m .

I model Ξ_{ni}^m as consisting of two elements. The first is a function of the total value of trade shipped by mode m between i and n , which I write as $(X_{ni}^m)^{\lambda_m}$, with $0 < \lambda_m < 1$. The parameter λ_m measures the sensitivity of congestion costs to trade volumes. A higher λ_m implies that trade costs respond more strongly to changes in bilateral trade flows by mode. The second element is a pair-specific component that can be interpreted as the capacity and or quality of the infrastructure used to ship goods, which I define as $I_{ni} = I_n \times I_i$. This approach is similar to that used in recent spatial models ([Fajgelbaum and Schaal, 2020](#); [Allen and Arkolakis, 2022](#); [Fuchs and Wong, 2024](#)). The total costs of moving a good with mode m from country i to country n are then given by:

$$d_{ni}^m = \delta_{ni}^m \Xi_{ni}^m = \delta_{ni}^m \frac{(X_{ni}^m)^\lambda}{I_n I_i}, \quad (6)$$

where δ_{ni}^m denotes the fundamental iceberg trade cost for mode m between i and n , and d_{ni}^m is the total cost of shipping goods using mode m . The mode-specific iceberg costs, δ_{ni}^m , capture all pair-specific determinants of transport costs other than infrastructure and congestion, and are assumed to be exogenous to the economy.

Since individual importers cannot influence market prices, I treat congestion costs as externalities that importers take as given when choosing the transport mode. In Appendix C.1, I show that under this assumption equation (4) remains unchanged.

For the rest of the paper, I assume that the capacity and quality of infrastructure are constant across countries and modes.¹⁶ At the end of this section, I show that, under this assumption, the level of infrastructure is not needed to compute counterfactuals in changes.

3.4 Production and Trade

The remainder of the model follows a standard Ricardian trade framework based on [Eaton and Kortum \(2002\)](#). I assume that a manufacturer's productivity in country n for producing good u is given by $z_n(u)$. As is common in this class of models, production efficiency is the realization of a random variable Z_n , which is independently distributed across countries and follows a Fréchet (Type II extreme value) distribution. In country n , the unit cost of the input bundle is therefore $c_n = w_n^\beta p_n^{1-\beta}$, where w_n and p_n denote, respectively, the wage level and the price index in country n .

Each country sources goods from the cheapest location. Thus, given the productivity distributions across nations, the price index in a location n is given by:

$$p_n = \gamma \phi_n^{-1/\theta} = \sum_{i=1}^N A_i (c_i d_{ni})^{-\theta}, \quad (7)$$

where A_i is the technology level, d_{ni} is the transport costs index, and θ is the shape parameter of the Fréchet distribution, which is also the elasticity of aggregate trade flows with respect to aggregate trade costs.

Given the price index in each location, the share of goods that country n buys from country i is given by:

$$\pi_{ni} = \frac{X_{ni}}{X_n^{Ma}} = \frac{A_n (w_n^\beta p_n^{1-\beta} d_{ni})^{-\theta}}{\Phi_n}. \quad (8)$$

3.5 Market Clearing

To close the model, I impose that the budget constraint holds in equilibrium. To better match the data, I allow each country to run trade deficits D_n and manufacturing trade deficits D_n^{Ma} . Following the national accounting framework in [Dekle et al. \(2007\)](#), I define GDP as $Y_n = w_n L_n$, while gross manufacturing output is given by $Y_n^{Ma} = X_n^{Ma} - D_n^{Ma}$. Since manufactured goods are used both as intermediate inputs and for final consumption, total demand for manufactures satisfies $X_n^{Ma} = \alpha_n X_n + (1 - \beta_n) Y_n^{Ma}$, where α_n denotes the share of manufactures in final demand and X_n is final absorption.

The market clearing condition imposes that final absorptions and production are equal in equilibrium

$$Y_n^{Ma} = \sum_{i=1}^N X_{ni} = \sum_{i=1}^N \pi_{in} X_i^{Ma},$$

¹⁶Endogenizing infrastructure investment would substantially increase the model's complexity and would require a dynamic setting that is outside the scope of this work.

solving for manufacturing production and balancing trade, the final budget constraint is:¹⁷

$$w_n L_n + D_n - \frac{1}{\alpha} D_n^{Ma} = \sum_{i=1}^N \pi_{ni} \left[w_i L_i + D_n - \frac{1-\beta}{\alpha} D_n^{Ma} \right]. \quad (9)$$

3.6 General Equilibrium

Equation (1) states that the final utility in country n depends on the consumption of each good u . We know that each good u can be sourced from destinations with lower prices; therefore, we can rewrite the utility as a function of the quantity imported from each origin:

$$U_n = \left(\int_0^1 \left[\sum_{n=1}^N q_{ni}(u) \right]^{\frac{\sigma-1}{\sigma}} du \right)^{\frac{\sigma}{\sigma-1}},$$

now it is possible to insert into this equation the lower nest defined by equation (29) which regulates how quantities from various origins are transported via different modes.

$$U_n = \left(\int_0^1 \left[\sum_{i=1}^N \left(\sum_{m=1}^M (q_{ni}^m)^{\frac{\eta-1}{\eta}} \right)^{\frac{\eta}{\eta-1}} \right]^{\frac{\sigma-1}{\sigma}} du \right)^{\frac{\sigma}{\sigma-1}}, \quad (10)$$

Then, given the technology, A , deficits, D, D^{Ma} , labor endowments, L , and transport costs, d_{ni}^m , an equilibrium is a vector of prices, p , wages, w , and bilateral transport costs, d , that satisfies the following system of equations:

share of expenditure

$$\pi_{ni} = \frac{X_{ni}}{X_n} = \frac{A_n (d_{ni} w_n^\beta p_n^{1-\beta})^{-\theta}}{\sum_{h=1}^N A_h (d_{nh} w_h^\beta p_h^{1-\beta})^{-\theta}},$$

price index

$$P_n = \left[\sum_{i=1}^N A_i (d_{ni} w_i^\beta p_i^{1-\beta})^{-\theta} \right]^{-1/\theta},$$

share of mode m between importer n and exporter i

$$\pi_{ni}^m = \frac{X_{ni}^m}{X_{ni}} = \frac{(d_{ni}^m)^{1-\eta}}{\sum_{m=1}^M (d_{ni}^m)^{1-\eta}},$$

transport cost index between importer n and exporter i

$$d_{ni} = \left[\sum_{m=1}^M (d_{ni}^m)^{1-\eta} \right]^{1/(1-\eta)},$$

¹⁷see Dekle et al. (2007) for an explicit derivation of the budget constraint

and a market clearing condition

$$w_n L_n + D_n - \frac{1}{\alpha} D_n^{Ma} = \sum_{i=1}^N \pi_{ni} \left[w_i L_i + D_n - \frac{1-\beta}{\alpha} D_n^{Ma} \right].$$

The main departure from standard Ricardian trade models is that d_{ni} is now jointly determined with wages and price indices in each country. Note that the usual parameter restriction $\theta > \sigma$ is still required to derive the bilateral trade shares π_{ni} . In addition, conditional on the choice of transport mode, an additional restriction $\eta > \sigma$ is needed. However, there is no restriction on the relationship between θ and η . This follows from the assumption that factory-gate prices are independent of the transport mode, so that transport costs are already determined once the origin of production is chosen.

3.7 System in Changes and Welfare

To compute welfare changes resulting from a shock to transport costs in a single mode, I apply the exact-hat algebra approach (Dekle et al., 2007). I assume that technology (A), labor endowments (L), aggregate trade deficits (D and D^{Ma}), and infrastructure (I) are constant across countries. I further assume that the shock takes the form of a change in transport costs for a generic mode $s \in M$. I define variables in changes as $\hat{x} = x'/x$, where x' denotes the post-shock value and x the pre-shock value.

The equations for the trade share between two countries, the price index, and the market clearing conditions can be written in changes as follows:

$$\hat{\pi}_{ni} = \frac{\left(\hat{d}_{ni} \hat{w}_i^\beta \hat{p}_i^{1-\beta} \right)^{-\theta}}{\sum_{h=1}^N \pi_{nh} \left(\hat{d}_{nh} \hat{w}_h^\beta \hat{p}_h^{1-\beta} \right)^{-\theta}} \quad (11)$$

$$\hat{P}_n = \left[\sum_{i=1}^N \pi_{ni} \left(\hat{d}_{ni} \hat{w}_i^\beta \hat{p}_i^{1-\beta} \right)^{-\theta} \right]^{-1/\theta} \quad (12)$$

$$\hat{w}_n Y_n + D_n - \frac{1}{\alpha} D_n^{Ma} = \sum_{i=1}^N \frac{\pi_{ni} \left(\hat{d}_{ni} \hat{w}_i^\beta \hat{p}_i^{1-\beta} \right)^{-\theta}}{\sum_{h=1}^N \left(\pi_{nh} \hat{d}_{nh} \hat{w}_h^\beta \hat{p}_h^{1-\beta} \right)^{-\theta}} \left[\hat{w}_n Y_n + D_n - \frac{1-\beta}{\alpha} D_n^{Ma} \right] \quad (13)$$

The crucial variable through which the shock propagates in the economy is the aggregate trade costs between countries \hat{d}_{ni} .

The change in the aggregate transportation cost, \hat{d}_{ni} , reflects both the direct change in costs for the affected mode and the induced price responses of other modes through congestion effects. In Appendix C.3, I show that the resulting impact on the transport cost index from a change $\hat{\delta}_{ni}^s$ can be written as:

$$\hat{d}_{ni} = \left[1 + \left((\hat{\delta}_{ni}^s (\hat{X}_{ni}^s)^\lambda)^{1-\eta} - 1 \right) \pi_{ni}^s + \sum_{m=1}^{s-1} \pi_{ni}^m \left((\hat{X}_{ni}^m)^{(\lambda)(1-\eta)} - 1 \right) \right]^{1/(1-\eta)}, \quad (14)$$

This formulation has two key features. First, it requires very little additional data relative to a standard quantitative trade model, namely the share of trade by mode between country pairs. Second, it implies that changes in aggregate trade costs differ across country pairs even when mode-specific cost changes are identical across routes. This occurs because the overall effect depends on the pre-shock modal shares. In this sense, these shares can be interpreted as measures of exposure to mode-specific shocks. Intuitively, the more intensively a mode is used along a given route, the more exposed that country pair is to increases in transport costs for that mode. These heterogeneous effects may amplify cross-country differences. For example, developing countries rely more heavily on sea transport, so an increase in sea transport costs would disproportionately affect economies that are already more vulnerable.

For a positive increase in mode- s transport costs, $\hat{\delta}ni^s > 1$, the aggregate transport cost $\hat{d}ni$ also increases, which lowers the overall level of trade between origin i and destination n . Given the structure of the model, I can derive welfare changes using the change in the domestic trade share, as is standard in this class of models ([Arkolakis et al., 2012](#)):

$$GT = \hat{\pi}_{nn}^{\left(\frac{1-\alpha}{\beta}\right)\left(-\frac{1}{\theta}\right)}. \quad (15)$$

Note that the welfare formula itself is unchanged, since the trade mechanism in the model mirrors that of standard quantitative models of international trade.

4 Estimation

In this section, I estimate the elasticity of substitution between transport modes, η , the key parameter of the model, together with the congestion parameter, λ . Identification of η relies on plausibly exogenous variation in mode-specific transport costs generated by large geopolitical and logistical disruptions. Specifically, I exploit the closure of Russian and Ukrainian airspace in 2022, which sharply increased air transport costs on Europe–Asia routes without directly affecting maritime transport. Because Eurostat data do not report transport prices, I complement this strategy by estimating the congestion parameter separately using a shift-share approach employing US data.

4.1 Substitution Between Transport Modes

This subsection estimates the elasticity of substitution between air and sea transport. The empirical strategy exploits shocks that generate differential changes in transport costs across modes while leaving product-level demand and bilateral trade relationships otherwise intact. The primary source of variation is the closure of Russian and Ukrainian airspace, which disproportionately affected air transport between Europe and Asia. As a robustness check and alternative source of identifying variation, I also exploit disruptions at U.S. West Coast ports in 2021, which primarily increased maritime transport costs.

Russian airspace is a critical corridor for Europe–Asia trade: approximately 36% of European extra-regional trade involves Asian partners.¹⁸ Importantly, this event affected only one transport mode at a time, providing clean variation in relative mode-specific costs. The airspace closure increased air transport costs due to longer flight times. This asymmetry allows the elasticity of substitution to be identified from changes in relative mode shares within narrowly defined country pairs and product categories.

A key identification assumption is that, conditional on fixed effects, this shock affects relative trade shares across modes only through its impact on relative transport costs. Several features of the empirical setting support this assumption. First, the timing of the sanctions was largely unanticipated, limiting the scope for anticipatory adjustments. Second, the shock is sufficiently persistent to induce firms to reorganize logistics rather than rely on short-run inventory smoothing, implying that the estimated responses reflect medium- to long-run substitution rather than transitory adjustment. Third, the shock did not involve direct physical destruction of transport infrastructure on the Europe–Asia trade corridor, ruling out supply-side disruptions that could differentially affect product availability across modes.

4.1.1 The Russian and Ukrainian Conflict and Airspace Closure

The Russian invasion of Ukraine in February 2022 led to a sharp deterioration in diplomatic and economic relations between Russia and several countries imposing sanctions, most notably the European Union. One immediate consequence was the mutual closure of airspace between the opposing blocs, while Ukrainian airspace was closed to civilian flights for security reasons. As a result, European carriers¹⁹ were forced to reroute flights to Asian destinations,²⁰ leading to substantial increases in flight times. I use these increases as a proxy for higher air transport costs.

Although geopolitical tensions had been rising since late 2021, the precise timing and scale of the invasion were widely viewed as unexpected. This limits the possibility that firms adjusted shipping modes in advance. Moreover, the conflict has persisted far longer than initially anticipated ([Zabrodskyi et al., 2022](#)), exhausting inventories and forcing firms to reoptimize transport decisions under the new routing constraints.

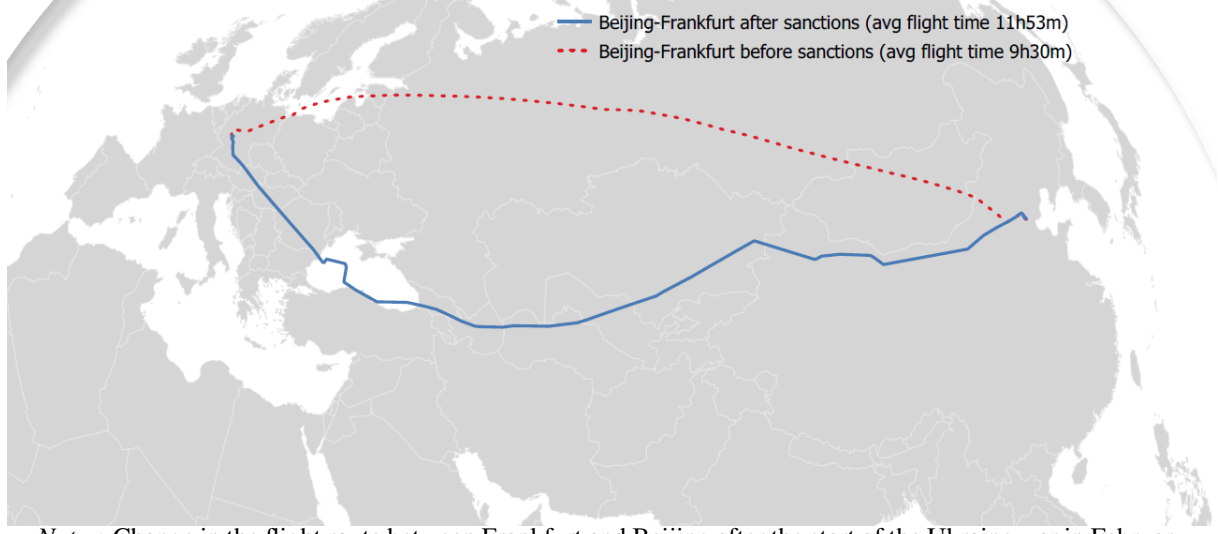
Importantly, sanctions-related trade restrictions, aside from airspace closures, are unlikely to bias the estimates. While sanctions may reduce overall trade volumes between certain country pairs, they do not differentially affect air and maritime transport costs and therefore should not mechanically shift relative mode shares. The identifying variation thus comes from within-country-pair changes in mode shares, holding fixed bilateral demand conditions and product composition. This structure supports a causal interpretation of the estimated elasticity

¹⁸Source: Eurostat.

¹⁹The restrictions also apply to other sanctioning countries, including Japan and South Korea. Chinese carriers, by contrast, continue to operate over Russian airspace.

²⁰Affected routes include flights to Japan, South Korea, China, and several destinations in Southeast Asia. Flights are typically diverted southward through Turkey, Central Asia, China, and Mongolia (source: Flight-tradar24).

Figure 3: Sanctions and Change in Flight Time



Notes: Change in the flight route between Frankfurt and Beijing after the start of the Ukraine war in February 2022. The flight time increases by 25 percent from 9h30mins to 11h53mins. Author's own calculation based on Flightradar24 data.

as reflecting substitution across transport modes in response to relative transport cost changes.

4.1.2 Empirical Strategy

In this section, I estimate the elasticity of substitution between transport modes with respect to transport costs within the same origin–destination pair. Specifically, I assess whether changes in relative mode-specific transport costs induce corresponding changes in relative trade shares by mode. More precisely, I estimate the empirical counterpart of equation (5) from the previous section.

My identification strategy relies on a difference-in-differences design that compares trade flows shipped by air and sea along routes affected by the war with those that were not, before and after the outbreak of the conflict in February 2022. This approach exploits the exogenous variation generated by the unexpected closure of Russian and Ukrainian airspace. Affected routes face higher air transport costs due to longer flight paths, which increase travel time and operating expenses.²¹ Figure 3 illustrates this mechanism. A flight from Frankfurt to Beijing operated by a European carrier, which previously crossed Russian airspace, must now take a longer detour, increasing flight time by more than two hours.

I use data on daily flights from January 2019 to December 2022, covering more than 1.8 million observations, from Strohmeier et al. (2021). These data are collected from ADS-B signals via the OpenSky platform.²² The key variables are the origin and destination airports and total flight time. I restrict the sample to international flights, excluding observations in which takeoff and landing occur within the same country, and thus focus on direct flights only. An underlying assumption is that commercial and cargo flights follow similar routes and have

²¹For example, a report from the Federal Aviation Administration indicates an average hourly operating cost of about USD 10,000 for a wide-body aircraft with more than 300 seats, over 90% of which consists of variable costs such as fuel and personnel. Fuel alone accounts for nearly 20% of total flight expenditures (FAA, 2022).

²²All aircraft are required to carry an ADS-B transponder while in flight.

comparable travel times.²³ I then compute monthly average flight times between country pairs, which I use as a proxy for air transport costs.

I define a route as an origin–destination country pair and classify it as affected if pre-war flight paths crossed either Russian or Ukrainian airspace. The treated group consists of routes between European countries and destinations in East and Southeast Asia. To identify affected routes, I rely on reports from the International Civil Aviation Organization (ICAO) and supplement them with manual verification using pre-war flight paths from Flightradar24.²⁴ The control group consists of North and South American countries that trade with Europe.²⁵

Finally, I restrict the sample to HS6 sectors for which at least 5% of trade value was shipped by both air and sea in 2019. This restriction allows me to focus on the intensive margin of adjustment rather than the extensive margin. In particular, I exploit variation within origin–destination–sector triplets that already use both modes, excluding cases where trade switches from a single mode to multiple modes. In Appendix A.3, I estimate a linear probability model to verify that the shock did not significantly affect the extensive margin by eliminating air transport for specific origin–destination–sector combinations.

To estimate the elasticity of substitution between air and sea transport following the increase in transport costs induced by the closure of Russian and Ukrainian airspace, I adopt a two-step approach. First, I estimate the effect of the sanctions on average flight times between European countries and Asian destinations:

$$\ln \text{FlightTime}_{niht} = \beta_1 \cdot \text{Post}_t \times \text{Treated}_{ni} + \mu_{nih} + \mu_{ht} + \epsilon_{niht}, \quad (16)$$

where FlightTime_{niht} denotes the average flight time between countries n and i in sector h at time t , Treated_{ni} is an indicator equal to one if the route is affected by the airspace closure, and Post_t equals one from February 2022 onward. The terms μ_{nih} and μ_{ht} denote origin–destination–sector and sector–time fixed effects, respectively. The coefficient of interest is β_1 , which captures the change in average flight time induced by the war.²⁶

In the second step, I estimate the impact of the sanctions on relative trade flows across transport modes. To isolate substitution across modes, I control for overall trade volumes within each origin–destination–sector triplet by taking the ratio of air to sea trade flows. This ratio nets out changes in total bilateral trade driven by common shocks and allows me to focus on changes in the relative modal composition of trade. Accordingly, the analysis does not aim to capture the overall effect of the war on trade volumes, but rather its effect on the allocation of trade between air and sea transport. In Appendix A.2, I separately examine the effect of the sanctions on trade flows by mode at the country-pair level.

²³I validate this assumption using Flightradar24, which reports real-time flight paths. Figure D.6 provides an example for flights between Beijing and Frankfurt.

²⁴Affected destinations include China and Hong Kong, Indonesia, Japan, South Korea, Malaysia, Myanmar, the Philippines, Singapore, Thailand, and Vietnam.

²⁵Because the affected routes are long-haul, I focus on air and sea transport only, as substitution toward land transport is limited. Moreover, land transport is not a feasible option for trade with the control group.

²⁶Because the sanctions do not affect sea travel times, this coefficient can be interpreted as the relative change in air transport costs with respect to sea transport.

I estimate the following equation:

$$\ln \left(\frac{X_{niht}^{Sea}}{X_{niht}^{Air}} \right) = \beta_2 \text{Post}_t \times \text{Treated}_{ni} + \mu_{nih} + \mu_{ht} + \epsilon_{niht}, \quad (17)$$

where $\ln (X_{niht}^{sea} / X_{niht}^{air})$ is the relative share of sea trade with respect to air trade between countries n and i in sector h at time t , Treated_{ni} , Post_t , μ_{nih} , and μ_{ht} are defined as above. The coefficient of interest is β_2 , which captures the change in sea trade flows with respect to air trade due to the increase in transport costs that followed the closure of the Russian airspace.

Finally, I calculate the ratio of these two coefficients to recover the elasticity of substitution between air and sea transport. This approach is referred to as the Wald-DiD estimator ([Wald, 1940](#); [Angrist and Pischke, 2009](#); [De Chaisemartin and d'Haultfoeuille, 2023](#))

$$\beta_{DiD} = \frac{E[\ln X_{niht} | \text{Post}_t \times \text{Treated}_{ni} = 1] - E[\ln X_{niht} | \text{Post}_t \times \text{Treated}_{ni} = 0]}{E[\ln \text{FlightTime}_{niht} | \text{Post}_t \times \text{Treated}_{ni} = 1] - E[\ln \text{FlightTime}_{niht} | \text{Post}_t \times \text{Treated}_{ni} = 0]}. \quad (18)$$

The intuition behind this approach is that, conditional on a set of controls, changes in average flight time between two countries provide a valid proxy for changes in air transport costs. These changes in flight time are therefore used as an instrument for air transport costs. The identifying assumption is that, once other factors are controlled for, the shock affects the relative trade shares between affected countries only through its impact on flight time.

This approach is equivalent to a two-stage least squares (2SLS) regression of the outcome $\ln (X_{niht}^{Sea} / X_{niht}^{Air})$ on the endogenous regressor $\ln \text{FlightTime}_{niht}$, using time variation (Post_t), group variation (Treated_{ni}), and their interaction as instruments ([De Chaisemartin and d'Haultfoeuille, 2018](#)).

Because this is a sharp difference-in-differences design in which treatment applies only to the treated group, the key identifying assumption is the validity of common trends. This sharp design is justified by the fact that exposure to the airspace closure is determined exogenously by countries' geographic locations.

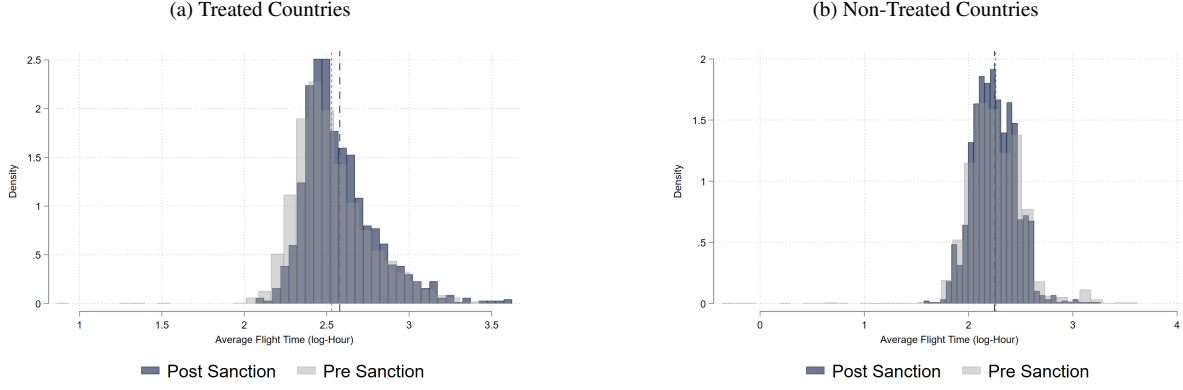
4.1.3 Identification Assumptions

In this section, I assess whether the results are driven by ex ante differences between treated and control routes or by pre-existing trends.

Before the war, the composition of trade flows by sector and average flight times are similar across affected and unaffected routes, as shown in Table [E.7](#). The unit of observation is the air trade flow or share between origin i and destination n at time t in sector h , where time is measured at the month–year level and sectors are defined at the 6-digit product level. The similarity of moments across the two groups suggests the absence of meaningful ex ante heterogeneity.

Figure [4](#) compares average flight times before and after the war for treated and control routes. The treated group, shown in the left panel, exhibits a clear increase in average flight time following the invasion, consistent with disruptions to air travel due to airspace closures and rerouting. In contrast, the control group displays stable average flight times throughout the

Figure 4: Change in the Average Flight Time



Notes: Panel (a) shows the average flight time before and after the sanctions that led to the closure of Russian airspace for treated country pairs. A country pair is classified as treated if it connects a European country with a destination in eastern or southern Asia. Panel (b) presents the corresponding statistics for the control group, which consists of country pairs linking European countries to North and South American destinations. The sample is based on monthly average flight times computed from approximately 1.8 million flight paths observed between January 2019 and December 2022, using AIS data from the OpenSky platform.

period.

Figure 5a shows no evidence of differential pre-treatment trends in flight time, with divergence occurring only after the outbreak of the war. In particular, average flight time rises sharply for treated routes following the invasion, while the control group continues along its pre-war trajectory. This pattern supports a causal interpretation in which the observed increase in flight time is driven by the war rather than by confounding factors.

Figure 5b shows that, after the conflict, treated routes experience an increase in sea trade relative to air trade, again with no pre-treatment differences in trends.²⁷ Notably, an anticipatory effect emerges, with air trade beginning to decline as early as February 2022, prior to the formal onset of hostilities. This suggests that economic agents adjusted their trade behavior in response to rising geopolitical tensions. In the robustness checks, I show that the results are robust to classifying February 2022 as part of the pre-treatment period.

4.1.4 Results

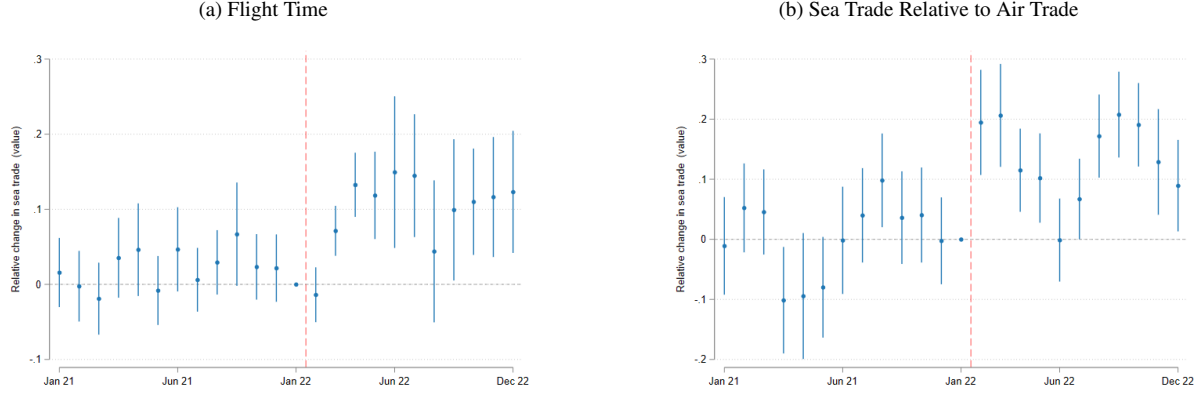
I find that the relative increase in air transport costs compared to sea transport on affected routes following the closure of Russian and Ukrainian airspace led to a substantial shift toward ocean shipping.

Table 1 reports the estimates of equations (16) and (17). Column (1) shows a significant increase in average flight time on treated routes relative to control routes following the outbreak of the war. The estimated coefficient β_1 is approximately 0.071, implying that average flight time rose by about 7% after the onset of the conflict.²⁸ Column (2) shows that this increase in flight time led to a substantial rise in sea trade relative to air trade. The estimated coefficient of

²⁷The same pattern holds when trade is measured in kilograms; see Figure D.7 in the appendix.

²⁸Given a pre-war average flight time of roughly 12.5 hours for treated routes, this corresponds to an increase of about one hour. Consistent with this magnitude, Chu et al. (2024) estimates that the closure of Russian airspace raised air transport costs by approximately 12%.

Figure 5: Event Studies



Notes: Panel (a) reports the event-study estimates based on equation (16) and shows no evidence of differential pre-trends in flight time between treated and control country pairs prior to the closure of Russian and Ukrainian airspace. Panel (b) reports the event-study estimates based on equation (17) and shows a significant increase in sea trade relative to air trade following the airspace closures for treated country pairs compared to the control group.

0.114 indicates that sea trade, measured in euros, increased by about 11% relative to air trade following the outbreak of the war.

The elasticity of substitution between transport modes is obtained using equation (18) by taking the ratio of the coefficient in column (2) to that in column (1). The estimation is implemented using the IV–2SLS strategy described above, and the results are reported in column (3) of Table 1. The estimates imply an elasticity of substitution between air and sea transport of approximately 1.599 in value terms. This implies that a 1% increase in air transport costs leads to a 1.6% increase in the share of trade shipped by sea. Using equation (5), this corresponds to an implied elasticity of substitution between transport modes of 2.6.

In column (4), I add freight prices for container shipping from Europe to destinations in the Americas and Asia as additional controls.²⁹ These controls account for potential movements in maritime transport prices over the period. The baseline results remain unchanged.

4.1.5 Product Heterogeneity

Product characteristics can play an important role in shaping the elasticity of substitution between transport modes. I explore this source of heterogeneity in two ways. First, I split the sample according to the ISIC Rev. 3 classification. Second, I partition the sample using several indicators that capture sectoral characteristics of traded goods, including unit value, temperature sensitivity, containerizability (Bernhofen et al., 2016), broad economic classification, and

²⁹These data are obtained from the Freightos Baltic Index (FBX) via the Eikon platform and consist of monthly averages of daily shipping indices for the following routes: Europe to the West Coast of South America, China to Northern Europe, China to Mediterranean Europe, Europe to the East Coast of North America, Europe to the East Coast of South America, Mediterranean Europe to China, Northern Europe to China, and the East Coast of North America to Europe.

Table 1: Substitution Between Modes of Transport

	(1) ln FlightTime	(2) ln (X^{Sea}/X^{Air})	(3) ln (X^{Sea}/X^{Air})	(4) ln (X^{Sea}/X^{Air})
In FlightTime			1.599 (0.697)	1.891 (0.745)
Post × Treated	0.071 (0.015)	0.114 (0.031)		
In Freight				0.030 (0.020)
$\hat{\eta}$			2.60	2.89
Obs.	2,821,847	2,821,847	2,821,847	2,821,847
Origin-Destination-HS6	✓	✓	✓	✓
Year-Month-HS6	✓	✓	✓	✓
F-Test			17.31	18.55
R^2	0.85	0.62		

Notes: Column (1) reports the estimates for regression (16). The dependent variable is the log average flight time between two country pairs. Column (2) reports the estimates for regression (17) where the dependent variable is the ratio, in euros, between sea and air trade between a country n and a country i in sector h in month t . Treated is a dummy that takes values 1 if the origin/destination country is in Asia and 0 otherwise. Post is a dummy that takes value 1 after the start of the war (February 2022) and 0 otherwise. The Wald-DiD estimator, equation (18), is calculated via 2SLS and is equivalent to the ratio of the coefficients in columns (1) and columns (2). The coefficient of column (3) can be interpreted as the elasticity of substitution between transport modes. Standard errors are clustered at the origin-destination-year level. Column (4) includes freight indexes from major European Ports to Asian and American destinations.

time sensitivity (Hummels and Schaur, 2013). Table E.8 reports descriptive statistics on the distribution of trade flows, in both value and volume, across these subgroups.

Table E.9 presents the 2SLS-IV estimates at the origin–destination–HS6 level, split by ISIC3 sector. Sectors exhibiting relatively high substitutability across transport modes include Textiles (3.58), Manufacturing (3.08), Communications (2.31), and Chemicals (1.83). These sectors tend to comprise goods that are relatively light and high value, making them suitable for shipment by both air and sea. However, splitting the sample into many sectors substantially reduces the number of observations in each subsample, which lowers precision for some estimates.

Table E.10 reports results based on product characteristics. Across BEC groups, consumption goods display the highest substitutability, with an elasticity of 2.66. As expected, non-containerizable goods exhibit the lowest elasticity at 0.81. There is no clear pattern regarding time sensitivity. In contrast, goods with lower trade costs exhibit the highest elasticity at 2.05, which is consistent with the fact that highly time-sensitive goods are rarely shipped by sea.

4.1.6 Robustness Checks

I conduct a series of robustness checks to ensure that the results are not driven by sample selection, timing choices, or unobserved characteristics of trade flows. Overall, the findings are robust across alternative samples, timing assumptions, and specifications that allow for within-sector adjustments.

Table E.11 shows that the results are robust when trade flows are measured in kilograms rather than euros. Table E.13 reports estimates of equation (18) using the full sample, rather

than restricting attention to goods with at least 5

In columns (4) and (5), I re-estimate the baseline specification using alternative clustering schemes for standard errors, at the origin–destination–HS6 level and at the origin–destination level, respectively. In column (6), I exclude landlocked European countries that cannot access ocean shipping directly.³⁰ The estimates remain in line with the baseline specification.

To assess whether goods shipped by different modes within the same HS6 category differ systematically in composition, I perform additional regressions on subsamples defined by the similarity of unit values across modes. For instance, high-quality wine may be transported by air, while lower-quality wine is shipped by sea. I therefore compute, for each origin–destination–sector–mode, the ratio of unit values and group observations into quartiles based on this ratio. The results, reported in Table E.12 in the Appendix, show that substitutability is highest when unit values across modes are similar (column (1)) and becomes insignificant when unit values differ substantially (column (4)). This pattern suggests that large differences in unit values reflect fundamentally different products, limiting substitution across modes.

To further rule out compositional changes within sectors, I re-estimate the baseline specification using the unit value ratio across modes as the dependent variable and also estimate the impact of the war separately for each mode. The results, reported in Table E.14, show that neither the unit value ratio nor unit values by mode respond significantly to increases in flight time. This evidence rules out changes in product quality as a driver of the results.

Finally, in Appendix A.3, I show that the number of transport modes used changes only marginally following the sanctions introduced after February 2022. This supports the focus on adjustments along the intensive margin, namely changes in relative trade shares across modes, rather than along the extensive margin of mode adoption.

4.1.7 Discussion

In this section, I show that the relative share of trade across transport modes within country pairs responds to changes in relative prices. I exploit the Russian–Ukrainian conflict and the subsequent closure of their airspace as a quasi-natural experiment that generated an exogenous increase in air transport costs. Using a difference-in-differences strategy that compares affected and unaffected routes, I find an elasticity of substitution between air and sea transport of approximately 2.6.

While this analysis identifies substitution from air to sea, less is known about substitution in the opposite direction. In Appendix B, I address this by using the 2021 disruptions at US West Coast ports as an alternative shock to transport modes. This setting allows me to estimate the elasticity of substitution from sea to air. Applying the same empirical strategy as in the baseline analysis, I find an elasticity that is both qualitatively and quantitatively close to 2.6. Together, these results provide support for the CES structure adopted in the model, as they suggest that a single parameter can reasonably capture substitution across transport modes.

³⁰These countries are Austria, the Czech Republic, Hungary, and Slovakia.

For comparison, the “naive” OLS regressions are reported in Table E.15 in the appendix and yield no significant effects. In that case, identification relies on short-run fluctuations in flight time between country pairs, which are unlikely to induce firms to adjust their transport mode. I therefore interpret the results in this section as reflecting long-run responses that are sufficiently large to prompt importers to switch transport modes in response to trade shocks.

To the best of my knowledge, this paper is among the first to estimate this elasticity in an international trade context. A related elasticity is estimated by [Fuchs and Wong \(2024\)](#) for US domestic trade, where the authors study substitution between rail and truck transport. Their estimates are smaller than those found here, which is consistent with differences in the modes considered. Earlier estimates in [Hummels and Schaur \(2013\)](#) are broadly in line with my findings, though somewhat larger, with maximum values around 6.

Standard trade models cannot account for these patterns. In classic gravity models, a single iceberg cost typically summarizes all bilateral trade costs between two countries. In contrast, this section shows that multiple transport modes can be used simultaneously along the same origin–destination route (Figure 2), and that the share of each mode responds systematically to changes in relative transport costs. Together, these findings provide new insights into the determinants of bilateral trade costs and how trade adjusts when those costs change.

In standard models, a change in trade costs is assumed to lead to a proportional reduction in trade flows. When multiple transport modes are available, however, part of this adjustment can occur through substitution across modes,³¹ partially mitigating the impact of higher costs. In Appendix A.2, I examine the effect of sanctions on trade flows by mode and in the aggregate. I find that air trade flows experienced a significant decline for affected origin–destination pairs, which was not fully offset by an increase in sea trade. As a result, aggregate trade flows also declined. Although bilateral sea trade flows decreased as well, this effect is not statistically significant. Overall, substitution across transport modes is insufficient to fully compensate for the increase in bilateral trade costs and uncertainty. This pattern is consistent with the predictions of the model developed in this paper.

4.2 Congestion

The model introduces a second parameter, λ , which captures the extent to which transport prices respond to changes in trade flows along a given origin–destination–mode. While this parameter is commonly used in spatial models of economic activity within countries ([Allen and Arkolakis, 2014, 2022; Fajgelbaum and Schaal, 2020; Fuchs and Wong, 2024](#)), this paper is among the first to incorporate it into a trade model. In this section, I estimate the congestion parameter for air and sea transport using a shift-share instrumental variable approach and show that the resulting estimates are consistent with those found in the literature.

³¹For example, by shifting toward relatively cheaper transport modes.

4.2.1 Strategy

In equation (6), transport costs between two countries depend not only on bilateral characteristics, such as distance or mode-specific prices, but also on how intensively a given mode is used along an origin–destination route. This creates a clear endogeneity problem if one were to estimate directly the effect of trade flows on transport prices, since prices and quantities are jointly determined. Identifying λ therefore requires a source of exogenous variation. Unfortunately, because Eurostat does not report transport prices, I cannot apply the strategy used in the previous section to estimate this parameter.

To address this issue, I employ a shift-share instrumental variable design using data from the US Census Bureau on US imports. Specifically, I instrument changes in trade flows to the United States for a given origin–mode–sector (HS6) with changes in trade flows of the same HS6 sector from all other origins exporting to the United States. As an alternative instrument, I also use European exports of the same HS6 sector to non-US destinations. Both shifters capture exogenous demand changes for specific goods along routes that should not directly affect transport prices for a given origin–mode shipping to the United States.

The corresponding shares are constructed as the HS6 share within an HS4 sector for each origin–mode, measured in 2012, the first year of the sample. This design identifies the congestion parameter λ_m as a share-weighted average of shocks that are plausibly exogenous ([Borusyak et al., 2025](#)). Moreover, the approach satisfies the key conditions for shift-share identification outlined by [Borusyak et al. \(2025\)](#): there are many independent shifters, and the shares sum to one.

I estimate the following equation:

$$\ln \text{freight}_{omkt} = \beta_\lambda \ln \text{Trade}_{omkt} + \mu_{oyk} + \mu_{ot} + \epsilon_{omkt} \quad (19)$$

Where $\ln \text{freight}_{omkt}$ is the average freight cost per kilo, computed as total charges divided by total weight, for importing an HS4 product k from origin o to the US using mode m in month t . $\ln \text{Trade}_{omkt}$ denotes trade flows, measured in kilos, for the same origin–product combination. The fixed effect μ_{oyk} captures total flows for product k from origin o in year y , while μ_{ot} controls for total flows from country o in month t . Together, these two sets of fixed effects control for total demand in a given year and sector, capturing general increases in US import demand by restricting identification to within-year demand shocks, and for total monthly US demand for goods from country o , which accounts for changes in tariffs or other shocks to aggregate bilateral trade. Standard errors are clustered at the origin level.

The parameter of interest is β_λ , which measures how transport costs respond to increases in trade flows at the origin–product–mode level. Theory predicts this parameter to be positive, as higher trade volumes generate congestion costs. However, equation (19) cannot be estimated directly due to endogeneity, since trade flows and transport costs are jointly determined. I therefore instrument changes in trade flows for a given origin–HS4–mode with a shift-share measure constructed from the sum of imports of HS6 products within the same HS4 category

from origins other than o in a given month, weighted by the importance of each HS6 product in total HS4 imports.

$$TradeShift_{omkt} = \sum_{h \in k} \sum_{j \neq o} s_{okm, 2012} X_{jhmt} \quad (20)$$

Where $s_{okm, 2012}$ denotes the share of HS6 product h within HS4 sector k imported from origin o using mode m in 2012, and X_{jhmt} is US imports of HS6 product h using mode m in month t from an origin $j \neq o$. As an alternative identification strategy, I also construct $TradeShiftEU_{omkt}$, which follows the same shift-share structure but uses exports of EU countries in a given HS6 sector to all destinations other than the United States as the shifter.

In the baseline analysis, I restrict the sample to the period 2014–2019 to ensure sufficient distance from the base year used to construct the shares and to avoid the COVID-19 period and the subsequent trade disruptions. As a robustness check, I show that the results are not sensitive to this sample restriction.

4.2.2 Results

An increase in trade flows leads to substantial increases in transportation costs for both air and sea transport. Table 2 reports the estimates of equation (19). Column (1) presents results from an OLS specification without an instrumental variable. The estimated coefficient β_λ is negative, contrary to theoretical predictions, which is likely due to endogeneity arising from the joint determination of quantities and prices. Column (2) reports estimates from equation (19) pooling across transport modes, thus capturing the aggregate average effect. Columns (3) and (4) report results separately for air and sea transport. In all three IV specifications, β_λ is positive and statistically significant, indicating that higher trade flows are associated with higher transportation prices. I interpret this positive relationship as reflecting congestion effects and increased demand for transportation services, which can generate delays and raise transport prices. The first-stage results and F-test statistics reported at the bottom of the table support the relevance and strength of the instruments.

The estimates in Table 2 imply an aggregate congestion parameter of 0.079. This value is consistent with existing estimates in the literature, such as [Fuchs and Wong \(2024\)](#), who find a port congestion elasticity of approximately 0.097, and [Carballo et al. \(2023\)](#), who show that processing delays increase transport prices by about 0.06. A key advantage of this approach is that it allows separate identification of congestion effects for air and sea transport. I find that air transport responds more strongly to increases in trade flows, with $\beta_\lambda = 0.097$, compared to sea transport, for which $\beta_\lambda = 0.062$. A plausible explanation is that air transport, which typically relies on smaller carriers and tighter capacity constraints, is more sensitive to demand spikes. This finding is important because it implies that, within the model presented in Section 3, trade flows by mode respond differently even to trade cost changes that are uniform across modes, such as tariffs, thereby introducing an additional margin of adjustment that is not captured in models with a single transport mode.

Table 2: Congestion and Transport Costs

	(1) ln $freight_{omkt}$ OLS	(2) ln $freight_{omkt}$ IV	(3) ln $freight_{omkt}$ IV Air	(4) ln $freight_{omkt}$ IV Sea
Log Weight	-0.162 (0.005)	0.079 (0.009)	0.097 (0.013)	0.062 (0.011)
Obs.	637,610	637,610	345,104	291,324
Origin-Year-HS4-Mode	✓	✓		
Origin-Year-HS4			✓	✓
Year-Month-Origin	✓	✓	✓	✓
First Stage		0.44	0.39	0.47
F-Test		1,401.97	871.29	1,273.41
R^2	0.81			

Notes: Column (1) reports the results of the OLS estimation for equation (19). Columns (2) to (4) instead report the Shift-share Iv strategy. The sample used consist of US imports from 2014 to 2019 at the monthly frequency from the US Census Bureau. Standard errors in parenthesis are clustered at the origin level.

4.2.3 Robustness

I perform a series of robustness checks to ensure that the results are not driven by the choice of instrument, the fixed effects, or the sample definition. Across all alternative specifications, the estimates remain quantitatively similar.

Table E.17 reports results using a shift-share instrument constructed from changes in exports from European countries to non-US destinations. Both the aggregate estimate and the mode-specific estimates are consistent with the baseline results. In this specification as well, air transport costs are more sensitive to changes in quantities than sea transport costs.

Table E.18 presents results under alternative fixed-effect structures. Columns (1) to (3) re-estimate the baseline specification using origin–product–quarter fixed effects instead of origin–product–year fixed effects. This specification sharpens identification by focusing on unexpected within-quarter increases in trade flows that may raise transport prices. Columns (4) to (6) instead include product–time fixed effects, μ_{kt} , which control for time-varying, product-specific shocks. Under both sets of fixed effects, the estimates remain close to the baseline in both magnitude and significance.

Finally, Table E.19 reports results for alternative samples. Columns (1) to (3) extend the sample to include the COVID-19 period and the subsequent recovery, while columns (4) to (6) expand the sample backward to include the years 2012 and 2013. In both cases, the results are very similar to the baseline, with the only notable difference being slightly lower estimated values of λ_m in the latter specification.

4.2.4 Discussion

In this section, I provide novel estimates of the congestion parameter λ_m that are consistent with the existing literature (Fuchs and Wong, 2024; Carballo et al., 2023). While this parameter is typically estimated for ocean or land transport, I also obtain estimates for air transport and

find them to be larger than those for other modes. Allowing congestion to differ by mode is important because it implies that shocks propagate differently across transport modes, even when their magnitudes are identical.

What this analysis does not capture, however, is the joint empirical effect of substitution across modes and congestion. This limitation is driven by data availability, as Eurostat does not report transport prices directly. In Appendix C.4, I show that the bias introduced in the estimation of η is small for the range of λ values estimated in this section and reported in the literature.

5 Quantitative Experiments

This section uses the model to evaluate policy counterfactuals that illustrate the role of transport mode substitution in transmitting cost shocks, comparing welfare responses with and without substitution to assess the importance of this adjustment margin. I also show that substitution plays a key role in shaping the emissions consequences of transport-related shocks.

I begin by considering two counterfactual scenarios: the closure of Russian–Ukrainian airspace and the closure of the Suez Canal.³² These scenarios are well suited to illustrating the role of substitution, as each primarily affects a single transport mode and highlights how geopolitical shocks can disrupt international trade through the transport sector.

I then show that substitution across transport modes is not only relevant for welfare outcomes but also central to understanding the environmental impact of trade. Mode-specific cost shocks alter the composition of trade across transport modes, with important implications for aggregate CO₂ emissions. To illustrate this channel, I analyze a policy experiment inspired by a recent International Maritime Organization (IMO) regulation aimed at reducing emissions from sea transport. By mandating lower vessel speeds, the regulation reduces effective shipping capacity and raises international sea transport costs.

The results reveal substantial heterogeneity in impacts across countries, underscoring the need for targeted policy responses. Differences in trade structure and modal dependence imply that countries are unevenly exposed to transport-related shocks. This heterogeneity highlights the importance of accounting for country-specific characteristics when designing trade policies, sanctions, or environmental regulations, and it reinforces the role of diversified trade routes and transport modes in enhancing economic resilience.

For each experiment, I compare outcomes from the full model with endogenous transport costs, described in Section 3, to those from a model that rules out substitution across transport modes. In the appendix, I also report results for a baseline model without congestion. The no-substitution case is implemented by imposing Cobb–Douglas expenditure shares over transport modes, while aggregate emissions are computed using trade weights from Comtrade, distances from UNCTAD, and mode-specific emissions intensities from [Shapiro \(2016\)](#). Changes in CO₂

³²The first experiment is motivated by the war in Ukraine, as discussed in the empirical section, and abstracts from other contemporaneous sanctions. The Suez Canal experiment is inspired by recent geopolitical instability in the Red Sea, which has increased travel distances and transport costs.

emissions should be interpreted as arising solely from adjustments in international transport, abstracting from changes in domestic production and internal transport emissions ([Copeland et al., 2022](#); [Sogalla et al., 2024](#)).

5.1 Taking the Model To the Data

Before turning to the estimation, I describe the data used to calibrate the model and the parameter values employed. Three key parameters govern how trade shocks propagate: the trade elasticity θ , the elasticity of substitution between transport modes along the same route η , and the congestion parameter λ_m . I set $m = 2$, corresponding to air and sea transport, the two modes used in the empirical analysis.

There is extensive literature on estimating θ in international trade ([Head and Mayer, 2014](#)). Since the focus of this paper is on substitution across transport modes, I set $\theta = 4$. Based on the estimates in Section 4, I set $\eta = 2.6$. For the congestion parameter, I allow it to differ by mode and set $\lambda = [0.097, 0.06]$ for air and sea transport, respectively. Finally, I take the expenditure shares α and β from [Eaton and Kortum \(2002\)](#).

Calibrating the remainder of the model requires data on trade by transport mode between countries, GDP, and trade balances. The sample is determined by the availability of bilateral trade flows by mode. European data are obtained from Eurostat, US data from the US Census Bureau, Japanese data from the Japan Customs Authority, ASEAN data from the ASEAN Secretariat, and Latin American and Caribbean data from the Inter-American Development Bank (IDB). I complement these sources with additional countries using data from the United Nations Statistical Division (UN Comtrade). The full list of countries is reported in Table E.21. I aggregate the European Union into a single entity, resulting in a final sample of 32 countries plus a residual rest-of-the-world (RoW) aggregate. China is the only country for which mode-specific data are unavailable; for China, I assume symmetric import and export shares by mode and use observed shares from partner countries.

For most countries, I use 2018 as the reference year. For ASEAN countries, data are only available for 2021 and 2022, so I use 2021 as the reference year for modal shares. I rely on import-reported data to construct bilateral import shares by mode and use export-reported flows to infer modal shares for China and the RoW.

Because the vast majority of international trade, in both value and quantity, is carried by air and sea, I restrict attention to these two modes. Land transport is largely confined to neighboring countries, generates many zero bilateral flows that are not explained by the model, and is inconsistently reported across data sources. This consideration also motivates aggregating the European Union into a single entity, as most extra-EU trade occurs via air and sea, while intra-EU trade is predominantly land-based.³³

I restrict the analysis to ISIC Rev. 3 manufacturing sectors: *Chemicals* (23–25), *Food* (15–16), *Machinery* (29–33), *Metals* (27–28), *Minerals* (26), *Other manufacturing* (36), *Tex-*

³³The UN Trade and Development Agency has recently released an experimental dataset on trade by mode of transport, but land transport suffers from similar reporting limitations.

tiles (17–19), *Vehicles* (34–35), and *Wood and paper* (20–22). This choice ensures consistency with the TradeProd database (Mayer et al., 2023), which I use to measure internal trade flows.³⁴

The mode-specific datasets are used solely to construct trade shares by transport mode. Aggregate trade flows are obtained from UN Comtrade to ensure consistency in product classification, measurement units, and trading partners. Since Comtrade does not systematically report internal trade, I use the TradeProd database to measure domestic flows. GDP data are taken from the World Bank, current account balances and manufacturing deficits from the IMF, and bilateral distances by mode from UNCTAD. Table E.20 summarizes the datasets used in the calibration.

Finally, I assume that internal trade is conducted using a single transport mode that is unaffected by external shocks. While this margin is unlikely to play a major role in the trade adjustment, as internal trade is typically carried by road or rail, it matters for the CO₂ calculations. In particular, this assumption implies that I cannot quantify changes in emissions from internal transport.

5.2 Transport Shocks, Substitution, and Policy Counterfactuals

This section uses the model to evaluate policy counterfactuals that isolate the role of transport mode substitution in propagating cost shocks. I consider three experiments that affect a single transport mode at a time: the closure of Russian-Ukrainian airspace, the permanent closure of the Suez Canal, and the introduction of the IMO23 regulation. For each experiment, I compare outcomes under the baseline model with endogenous substitution to a counterfactual model in which modal shares are fixed.

5.2.1 Closure of Russian–Ukrainian Airspace

The war in Ukraine led to the closure of Russian and Ukrainian airspace for European carriers.³⁵ I model this event as a permanent 7% increase in air transport costs on routes connecting Europe and Asia, consistent with the estimates in Section 4 and the evidence in Chu et al. (2024).

Table 3 Panel (a) reports average welfare changes for countries directly exposed to the shock.³⁶ Allowing for substitution reduces, on average, welfare losses by about 4.3% (0.004 percentage points) relative to a model with fixed modal shares. While these numbers may appear small, they are in line with the magnitude of the effect of a major trade deal between developed economies (Caliendo and Parro, 2015, 2022). Moreover, at the National-aggregate level, even small changes in the percentage of welfare can have significant economic implications. The mechanism is a partial reallocation toward sea transport: the sea-air trade ratio increases by roughly 10%, closely matching the empirical estimates in Table 1. Welfare losses

³⁴Because the source data are reported in the Harmonized System classification, I use concordance tables from the UN WITS database to map products across classifications.

³⁵See Section 4.1.1 for institutional details. Other sanctions are abstracted to isolate the transport cost shock.

³⁶Table E.22 contains the detailed results for all the countries.

are heterogeneous across countries and are larger for those with greater pre-shock reliance on air transport, consistent with equation (14), as can be seen in Figure 6.

Substitution also affects emissions. While longer flight paths increase aviation emissions, the shift toward maritime transport mitigates total CO₂ emissions in Europe relative to the no-substitution benchmark, Figure 7. Asia experiences emission reductions in both models due to trade reorientation toward closer partners.

Figure 6: Closure of Russian-Ukrainian Airspace: Welfare and Air Share

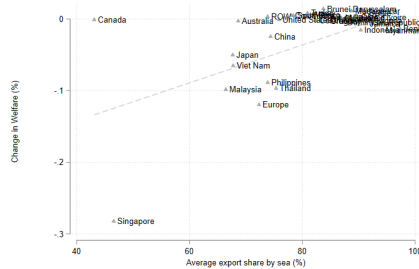


Figure 7: Closure of Russian-Ukrainian Airspace: Change in Emissions

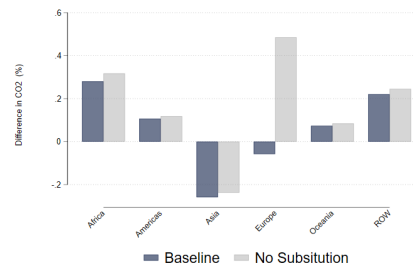


Figure 8: Closure of the Suez Canal: Welfare by Region

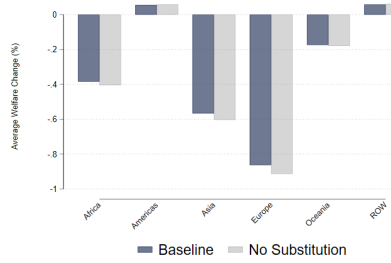


Figure 9: Closure of the Suez Canal: Change in Emissions

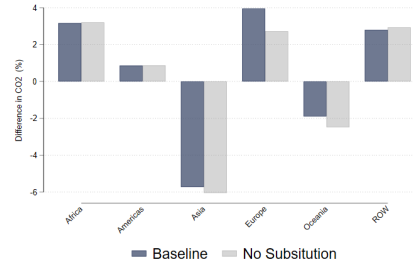


Figure 10: IMO23: Change in Welfare and Air Share

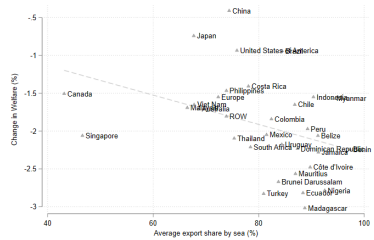
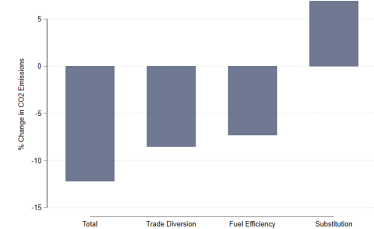


Figure 11: IMO23: Change in Emissions



5.2.2 Permanent Closure of the Suez Canal

The Suez Canal handles roughly 20% of global seaborne trade (Unctad, 2024). Motivated by recent disruptions in the Red Sea, I simulate a permanent closure by increasing sea transport costs along affected routes using the distance-based estimates in Feyrer (2019).

Table 3 Panel (b) shows that the average welfare losses in affected countries are approximately 0.8%, with substitution mitigating losses by roughly 6% relative to the no-substitution model.³⁷ Europe and Asia are the most affected, while countries in the Americas benefit from

³⁷Table E.23 contains the detailed results for all the countries.

Table 3: Welfare and Emissions Effects of Transport Policy Counterfactuals

	Baseline Model	No Substitution
<i>Panel A. Russian–Ukrainian Airspace Closure</i>		
Average welfare change (%)	-0.0858 (+4.31)	-0.0893
<i>Panel B. Suez Canal Closure</i>		
Average welfare change (%)	-0.808 (+6.23)	-0.857
<i>Panel C. IMO 2023 Policy</i>		
Average welfare change (%)	-1.907 (+2.20)	-1.947
Average CO ₂ change (%)	-12.53 (+18.2)	-15.40

Notes: The table reports average percentage changes relative to the initial equilibrium for countries directly affected by each counterfactual. The *Baseline Model* corresponds to the full model described in Section 3. The *No Substitution* specification shuts down substitution across transport modes (Section C.6). In *Panel (a)* the Russian–Ukrainian airspace closure is modeled as a permanent 7% increase in air transport costs on routes connecting Europe and Asia. Numbers in parentheses report the percentage difference relative to the no-substitution benchmark. *Panel (b)* studies the permanent closure of the Suez Canal. The change of distance is modeled based on Feyrer (2019). In *Panel (c)* the IMO23 policy is simulated by increasing sea transport costs by 10% and by decreasing CO₂ emissions in sea transport by 7.3%.

general equilibrium trade diversion (Figure 8).

In contrast to the airspace closure, substitution here amplifies emissions. Higher sea costs induce a shift toward air transport, which is substantially more carbon intensive, leading to higher imported CO₂ emissions in many regions despite lower aggregate trade (Figure 9).

5.2.3 Environmental Policy: IMO23

The final experiment studies the IMO23 regulation, introduced by the International Maritime Organization in July 2023, which aims to reduce carbon emissions from sea trade (MEPC, 2023). It includes measures addressing the specific characteristics of ships and carrier speeds. Lugovskyy et al. (2023) estimate that this measure likely causes an 8% decrease in shipping capacity across various countries, potentially increasing transport costs by the same magnitude. The authors also argue that this measure could lead to increased air transport usage, which, being more polluting, could potentially reverse the intended policy outcomes and increase total emissions. However, their model and applications consider only trade with the United States.

This experiment extends their analysis to a multi-country framework. Drawing on their findings, IMO23 is modeled here as an increase in sea transport costs due to capacity loss in the sector. Furthermore, this study assumes that pollution is generated only through transport and not by production itself, a simplification compared to works such as Cristea et al. (2013) and Shapiro (2016).

I simulate the measure as a 10% increase in sea transport costs, while the counterfactual CO₂ production level per ton-kilometer is 7.3% lower for sea trade and unchanged for air trade.³⁸

³⁸This figure is derived from Lugovskyy et al. (2023), which indicates it as the estimated fuel efficiency gain

The underlying assumption is that this analysis estimates the long-run impact of the policy while holding infrastructure constant.

All countries suffer from welfare losses since the increase in maritime costs affects all country-pairs. In Table 3 Panel (c), the average loss is around 0.05 percentage points lower (around 2.2%) in the model with substitution than in the model with fixed shares, highlighting that substitution can play an important role in mitigating mode-specific shocks.³⁹

Given that the policy increases costs for all countries in the same way, but different countries have different exposures to maritime costs, the effect is heterogeneous across the world. In particular, Figure 10 shows how lower- and middle-income countries incur larger welfare losses due to their more intense use of ocean trade. Therefore, this policy disproportionately affects countries with an already more fragile economy.

However, substitution substantially weakens the environmental effectiveness of the policy. The average difference in emissions with and without substitution is around 18% (3 percentage points). In Figure 11, I show that switching from maritime trade to air trade almost entirely off-sets the reduction in emissions achieved via the policy. Therefore, the lower level of CO₂ is achieved almost entirely through lower trade given the higher costs.

Across all three experiments, substitution across transport modes plays a quantitatively meaningful role in shaping welfare and environmental outcomes. While substitution mitigates welfare losses from mode-specific cost shocks, it can substantially undermine the effectiveness of environmental policies targeting a single transport mode. These results highlight the importance of accounting for modal substitution when evaluating trade shocks and designing transport and climate policy.

6 Conclusion

This paper studies how substitution across transport modes shapes the trade, welfare, and environmental consequences of mode-specific transport cost shocks. Motivated by recent disruptions to air and maritime transport, I develop a quantitative multicountry trade framework that allows agents to choose among multiple transport modes, subject to endogenous congestion costs. The model nests standard Ricardian gravity structures while introducing a new margin of adjustment—mode substitution—that is absent from much of the existing trade literature.

Empirically, I provide novel estimates of the elasticity of substitution between transport modes using quasi-natural experiments arising from the closure of Russian airspace and disruptions at U.S. West Coast ports. The results indicate substantial substitutability across modes, with meaningful heterogeneity across products. I also estimate congestion elasticities for both maritime and air transport, documenting that congestion plays an important role in shaping equilibrium transport costs.

Counterfactual simulations show that allowing for transport mode substitution significantly

for the US.

³⁹Table E.24 reports the disaggregated results by country.

attenuates welfare losses from mode-specific increases in transport costs, but also alters their distribution across countries depending on initial mode reliance. At the same time, substitution across modes has important implications for emissions: when one transport mode becomes more costly, trade flows may reallocate toward alternatives with higher carbon intensity, partially offsetting intended environmental gains.

From a policy perspective, these findings highlight the importance of evaluating trade, infrastructure, and environmental policies within a framework that explicitly accounts for transport mode substitution. Mode-specific interventions, such as infrastructure investments, canal closures, sanctions, or regulations targeting emissions in a single transport sector, can have unintended effects once firms adapt their transport choices. Ignoring this adjustment margin may lead to an overestimation of welfare losses from transport disruptions and an overstatement of the emissions reductions associated with mode-specific climate policies. More broadly, policies aimed at improving the resilience and sustainability of global trade are likely to be more effective when designed in a coordinated manner across transport modes, taking into account congestion, substitution, and heterogeneous exposure across countries.

References

- Al-Malk, A., Maystadt, J.-F., and Zanardi, M. (2024). The gravity of distance: Evidence from a trade embargo. *Journal of Economic Geography*.
- Allen, T. and Arkolakis, C. (2014). Trade and the topography of the spatial economy. *Quarterly Journal of Economics*, 129(3):1085–1140.
- Allen, T. and Arkolakis, C. (2022). The welfare effects of transportation infrastructure improvements. *Review of Economic Studies*, 89(6):2911–2957.
- Allen, T., Arkolakis, C., and Takahashi, Y. (2020). Universal gravity. *Journal of Political Economy*, 128(2):393–433.
- Anderson, S. P., De Palma, A., Thisse, J.-F., et al. (1987). The CES is a discrete choice model? *Economics Letters*, 24(2):139–140.
- Angrist, J. D. and Pischke, J.-S. (2009). *Mostly harmless econometrics: An empiricist's companion*. Princeton University Press.
- Arkolakis, C., Costinot, A., and Rodríguez-Clare, A. (2012). New trade models, same old gains? *American Economic Review*, 102(1):94–130.
- Asturias, J. (2020). Endogenous transportation costs. *European Economic Review*, 123:103366.
- Bernhofen, D. M., El-Sahli, Z., and Kneller, R. (2016). Estimating the effects of the container revolution on world trade. *Journal of International Economics*, 98:36–50.

- Besedeš, T., Chu, J., and Murshid, A. P. (2024). Fly the unfriendly skies: The role of transport costs in gravity models of trade. *Journal of International Economics*, 152:103994.
- Borusyak, K., Hull, P., and Jaravel, X. (2022). Quasi-experimental shift-share research designs. *The Review of economic studies*, 89(1):181–213.
- Borusyak, K., Hull, P., and Jaravel, X. (2025). A practical guide to shift-share instruments. *Journal of Economic Perspectives*, 39(1):181–204.
- Brancaccio, G., Kalouptsidi, M., and Papageorgiou, T. (2020). Geography, transportation, and endogenous trade costs. *Econometrica*, 88(2):657–691.
- Caliendo, L. and Parro, F. (2015). Estimates of the trade and welfare effects of NAFTA. *Review of Economic Studies*, 82(1):1–44.
- Caliendo, L. and Parro, F. (2022). Trade policy. *Handbook of International Economics*, 5:219–295.
- Campante, F. and Yanagizawa-Drott, D. (2018). Long-range growth: Economic development in the global network of air links. *Quarterly Journal of Economics*, 133(3):1395–1458.
- Carballo, J., Graziano, A., Schaur, G., and Martincus, C. V. (2014). The heterogeneous costs of port-of-entry delays. *Documento de discusión del BID*, 351.
- Carballo, J., Graziano, A., Schaur, G., and Volpe Martincus, C. (2023). Import processing and trade costs. IDB Working Paper Series IDB-WP-01454, Inter-American Development Bank, Washington, DC.
- Chu, C., Zhang, H., Zhang, J., Cong, L., and Lu, F. (2024). Assessing impacts of the russia-ukraine conflict on global air transportation: From the view of mass flight trajectories. *Journal of Air Transport Management*, 115:102522.
- Coşar, K. and Thomas, B. (2021). The geopolitics of international trade in Southeast Asia. *Review of World Economics*, 157(1):207–219.
- Copeland, B., Shapiro, J., and Taylor, M. (2022). *Handbook of International Economics*, chapter on globalization and the environment.
- Cotterlaz, P. and Vicard, V. (2023). Why origin matters in trade data. *CEPII Working Paper*.
- Cristea, A., Hummels, D., Puzzello, L., and Avetisyan, M. (2013). Trade and the greenhouse gas emissions from international freight transport. *Journal of Environmental Economics and Management*, 65(1):153–173.
- Cristoforoni, E., Errico, M., Rodari, F., and Tolva, E. (2025). Oligopolies in trade and transportation: Implications for the gains from trade.

- De Chaisemartin, C. and d'Haultfoeuille, X. (2018). Fuzzy differences-in-differences. *Review of Economic Studies*, 85(2):999–1028.
- De Chaisemartin, C. and d'Haultfoeuille, X. (2023). Two-way fixed effects and differences-in-differences with heterogeneous treatment effects: A survey. *Econometrics Journal*, 26(3):C1–C30.
- Dekle, R., Eaton, J., and Kortum, S. (2007). Unbalanced trade. *American Economic Review*, 97(2):351–355.
- Do, A., Ganapati, S., Wong, W. F., and Ziv, O. (2024). Transshipment hubs, trade, and supply chains.
- Eaton, J. and Kortum, S. (2002). Technology, geography, and trade. *Econometrica*, 70(5):1741–1779.
- Evans, C. L. and Harrigan, J. (2005). Distance, time, and specialization: Lean retailing in general equilibrium. *American Economic Review*, 95(1):292–313.
- FAA (2022). Benefit-Cost Analysis. *Chapter 4 Aircraft Operating Costs*.
- Fajgelbaum, P. D. and Schaal, E. (2020). Optimal transport networks in spatial equilibrium. *Econometrica*, 88(4):1411–1452.
- Felbermayr, G., Peterson, S., and Wanner, J. (2023). Structured literature review and modelling suggestions on the impact of trade and trade policy on the environment and the climate. *DG TRADE Chief Economist Notes*, (2022-3).
- Feyrer, J. (2019). Trade and income—Exploiting time series in geography. *American Economic Journal: Applied Economics*, 11(4):1–35.
- Feyrer, J. (2021). Distance, trade, and income—The 1967 to 1975 closing of the Suez Canal as a natural experiment. *Journal of Development Economics*, 153:102708.
- Fuchs, S. and Wong, W. F. (2024). Multimodal transport networks. *CEPR Discussion Paper No. DP19531*.
- Hansen-Lewis, J. and Marcus, M. M. (2022). Uncharted waters: Effects of maritime emission regulation. *National Bureau of Economic Research*.
- Harrigan, J. (2010). Airplanes and comparative advantage. *Journal of International Economics*, 82(2):181–194.
- Head, K. and Mayer, T. (2014). Gravity equations: Workhorse, toolkit, and cookbook. In *Handbook of international economics*, volume 4, pages 131–195. Elsevier.

- Hu, P., Schmitt, R. R., Schwarzer, J., Moore, W. H., et al. (2021). Transportation statistics annual report 2021. *United States Department of Transportation. Bureau of Transportation Statistics*.
- Hummels, D. (2007). Transportation costs and international trade in the second era of globalization. *Journal of Economic Perspectives*, 21(3):131–154.
- Hummels, D., Lugovskyy, V., and Skiba, A. (2009). The trade reducing effects of market power in international shipping. *Journal of Development Economics*, 89(1):84–97.
- Hummels, D. and Skiba, A. (2004). Shipping the good apples out? an empirical confirmation of the alchian-allen conjecture. *Journal of Political Economy*, 112(6):1384–1402.
- Hummels, D. L. and Schaur, G. (2010). Hedging price volatility using fast transport. *Journal of International Economics*, 82(1):15–25.
- Hummels, D. L. and Schaur, G. (2013). Time as a trade barrier. *American Economic Review*, 103(7):2935–59.
- IATA (2022). Air cargo market analysis. July 2022.
- IATA (2025). Air cargo market analysis. Press Release No. 46.
- Ignatenko, A. (2020). Price discrimination in international transportation: Evidence and implications.
- Jaworski, T., Kitchens, C., and Nigai, S. (2023). Highways and globalization. *International Economic Review*, 64(4):1615–1648.
- Ko, J.-w., Nigai, S., and Truax, A. (2025). Sectoral transport mode elasticities and international trade. Technical report.
- Ludwig, P. (2025). Can unilateral policy decarbonize maritime trade? Technical report, CESifo Working Paper.
- Lugovskyy, V., Skiba, A., and Terner, D. (2023). Unintended consequences of environmental regulation of maritime shipping: Carbon leakage to air shipping. Available at SSRN 4432161.
- Lux, M. (2011). Defying gravity: The substitutability of transportation in international trade.
- Mayer, T., Santoni, G., and Vicard, V. (2023). *The CEPII Trade and Production Database*. CEPII.
- MEPC, R. (2023). 2023 IMO strategy on reduction of GHG emissions from ships.
- Micco, A. and Serebrisky, T. (2006). Competition regimes and air transport costs: The effects of open skies agreements. *Journal of International Economics*, 70(1):25–51.

- Mundaca, G., Strand, J., and Young, I. R. (2021). Carbon pricing of international transport fuels: Impacts on carbon emissions and trade activity. *Journal of Environmental Economics and Management*, 110:102517.
- Rich, J., Kveiborg, O., and Hansen, C. O. (2011). On structural inelasticity of modal substitution in freight transport. *Journal of Transport Geography*, 19(1):134–146.
- Sandkamp, A., Stamer, V., and Yang, S. (2022). Where has the rum gone? the impact of maritime piracy on trade and transport. *Review of World Economics*, 158(3):751–778.
- Santamaría, M., Ventura, J., and Yeşilbayraktar, U. (2023). Exploring European regional trade. *Journal of International Economics*, page 103747.
- Shapiro, J. S. (2016). Trade costs, CO₂, and the environment. *American Economic Journal: Economic Policy*, 8(4):220–254.
- Shapiro, J. S. (2021). The environmental bias of trade policy. *Quarterly Journal of Economics*, 136(2):831–886.
- Söderlund, B. (2020). The importance of business travel for trade: Evidence from the liberalization of the Soviet airspace. *Available at SSRN 4220701*.
- Sogalla, R., Wanner, J., and Watabe, Y. (2024). New trade models, same old emissions?
- Strohmeier, M., Olive, X., Lübbe, J., Schäfer, M., and Lenders, V. (2021). Crowdsourced air traffic data from the OpenSky Network 2019–2020. *Earth System Science Data*, 13(2):357–366.
- Unctad (2024). Navigating troubled waters: Impact to global trade of disruption of the shipping routes in the Red Sea, Black Sea and Panama Canal. *Unctad Rapid Assessment*.
- Wald, A. (1940). The fitting of straight lines if both variables are subject to error. *The Annals of Mathematical Statistics*, 11(3):284–300.
- Wong, W. F. (2022). The round trip effect: Endogenous transport costs and international trade. *American Economic Journal: Applied Economics*, 14(4):127–66.
- Zabrodskyi, M., Watling, J., Danylyuk, O. V., and Reynolds, N. (2022). *Preliminary Lessons in Conventional Warfighting from Russia's Invasion of Ukraine, February-July 2022*. Royal United Services Institute for Defence and Security Studies London.

A Data Appendix

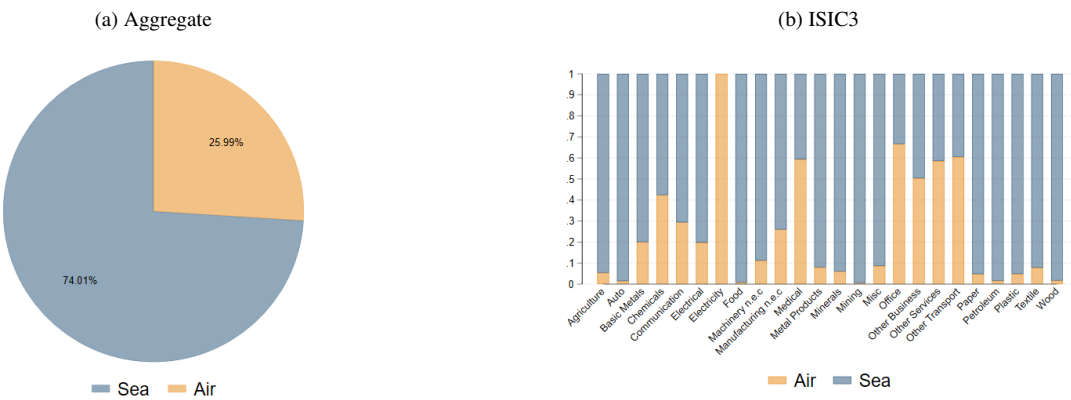
A.1 US Statistics

US Census Bureau data on U.S. imports are widely used in the literature to study transport mode choice in international trade (Hummels, 2007; Hummels and Schaur, 2013) and therefore provide a natural benchmark for assessing the representativeness of the Eurostat data used in the main analysis.

As in European trade, air transport accounts for a substantial share of U.S. imports. Approximately 25 percent of the total import value is shipped by air (Figure A.12), a pattern that holds across HS sections.

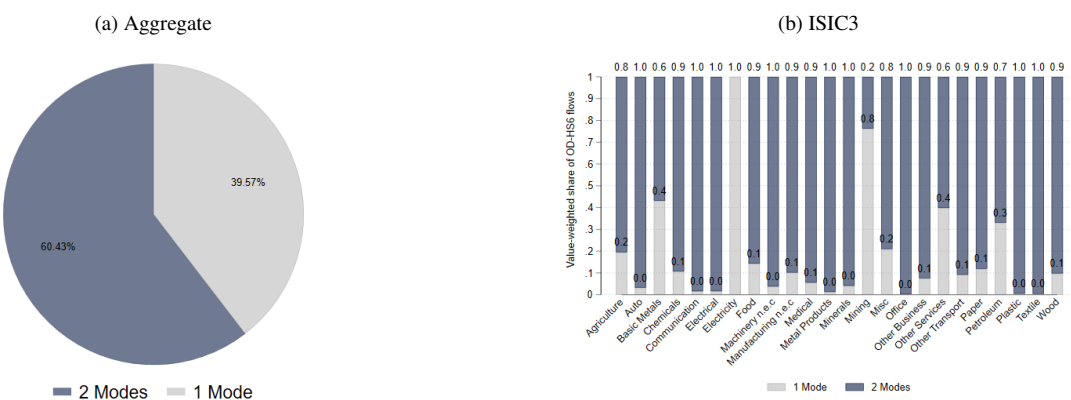
Consistent with the European evidence, Figure A.13 shows that roughly 60 percent of origin–destination–sector triplets use both air and sea transport. Although this share varies across HS sections, the simultaneous use of both transport modes is observed in all sectors.

Figure A.12: Transport Mode Share of Trade: US Data



Notes: Panel (a) reports the aggregate share of trade in dollars by mode of transport. Panel (b) reports the aggregate share of trade in dollars by mode of transport by HS Section. The sample consists of US trade flows in euros in 2019, collected from US Census Bureau.

Figure A.13: Number of Modes Used per Origin-HS6: US Data



Notes: Panel (a) reports percentage of origin-product that use two modes of transport. Panel (b) reports percentage of origin-product that use two modes of transport by HS Section. The sample consists of US trade flows in euros in 2019, collected from US Census Bureau.

A.2 Aggregate Effect of the Airspace Closure

In this section, I examine the effect of the closure of Russian and Ukrainian airspace on trade flows by transport mode. As shown in the main text, the airspace closure led to a significant increase in average flight times between European countries and Asian destinations. I use this increase in flight time as a proxy for higher transport costs for air-freighted goods. I then document that the rise in air transport costs resulted in a decline in the relative share of air transport compared with sea transport. I analyze these effects first at the mode level and then for aggregate trade flows.

To quantify the impact of the airspace closure on trade flows, I estimate the following specification:

$$\ln X_{nihtm} = \beta, \text{Post}_t \times \text{Treated}_{ni} + \mu_{nih} + \mu_{ht} + \epsilon_{nihtm}, \quad (21)$$

where $\ln X_{nihtm}$ denotes the value of trade between exporter i and importer n in sector h at time t , shipped using transport mode m . The variables Treated_{ni} , Post_t , and the fixed effects μ_{nih} and μ_{ht} are defined as in the main text. I first estimate equation (21) separately for air and sea transport, and then for total trade aggregated across modes.

The coefficient of interest, β , captures the change in trade flows induced by the increase in transport costs following the closure of Russian airspace.

Table A.4: Increase in air transport: aggregate effect

	(1) Air	(2) Sea	(3) All	(4) Aggregate
Post \times Treated	-0.160*** (0.018)	-0.038 (0.043)	-0.099*** (0.023)	-0.091*** (0.024)
Observations	2,472,709	2,472,709	4,958,592	2,472,709
R-squared	0.808	0.772	0.619	0.860
Origin-destination-HS6	Y	Y	Y	Y
Year-Month-HS6	Y	Y	Y	Y
Transport-HS6	N	N	Y	N

Notes: This table reports the results of the estimation of equation (21). In column (1) trade flows are by air and in column (2) are via sea. Column (3) reports the estimate for both which allow to include transport-date fixed effects (μ_{mt}). Column (4) report the results for the aggregate trade flows collapsed at the origin-destination-sector level. Standard errors are clustered at the origin-destination level. All the estimations are performed as OLS. Significance levels: *** p<0.01, ** p<0.05, * p<0.1.

Table A.4 reports the results from estimating equation (21).⁴⁰ Column (1) reports estimates for air shipments, while column (2) reports estimates for maritime shipments. The results show that the airspace closure led to a significant decline in trade flows transported by air. The estimated effect on maritime trade is negative but not statistically significant.

Columns (3) and (4) report the effects on aggregate trade flows across transport modes. The aggregate effect is negative and statistically significant, indicating that the increase in transport costs reduced total trade between affected country pairs. This finding is consistent with the

⁴⁰The table reports results for trade flows measured in euros. The results are quantitatively similar when trade flows are measured in kilograms; these estimates are available upon request.

interpretation that substitution across transport modes, while present, is insufficient to fully offset the increase in bilateral transport costs induced by the airspace closure.

A.3 Airspace Closure and Number of Modes Used

In this section, I examine the effect of the closure of Russian airspace on the number of transport modes used by affected country pairs relative to the control group. The objective is to show that the primary impact of the sanctions operates through changes in mode shares rather than through the abandonment of air transport altogether.

To study this margin, I estimate the following linear probability model:

$$\text{TwoMode}_{niht} = \beta, \text{Post}_t \times \text{Treated}_{ni} + \mu_{nh} + \mu_{ht} + \epsilon_{niht}, \quad (22)$$

where TwoMode_{niht} is an indicator equal to one if exporter i and importer n in sector h at time t use both air and sea transport, and zero otherwise. The variables Treated_{ni} , Post_t , and the fixed effects μ_{nh} and μ_{ht} are defined as in the main text. The coefficient of interest, β , captures the effect of the airspace closure on the probability that a given origin–destination–sector triplet uses both transport modes.

Table A.5 reports the estimation results. The closure of Russian and Ukrainian airspace had no economically meaningful effect on the number of transport modes used by affected origin–destination–sector triplets relative to non-affected ones. Although the estimated coefficient is negative and statistically significant, it corresponds to a reduction in probability of only 1.5 percentage points. This magnitude suggests that the relevant margin of adjustment is the intensive margin, changes in the relative shares of air and sea transport, rather than the extensive margin, defined as the number of modes used.

Table A.5: Increase in air transport: Linear Probability Model

	(1)
	Number of Modes
Post × Treated	-0.015** (0.006)
Observations	6,869,061
R-squared	0.603
Origin-destination-HS6	Y
Year-Month-HS6	Y

Notes: This table reports the results of the estimation of equation (22). The dependent variable TwoMode_{niht} is a dummy that takes value 1 if country n and i in sector h at time t used two modes and 0 otherwise. Standard errors are clustered at the origin-destination level. All the estimations are performed as OLS. Significance levels: *** p<0.01, ** p<0.05, * p<0.1.

B US West Coast Port Disruption

This section examines the 2021 U.S. West Coast port disruption as an alternative shock to transport modes and uses it to estimate the elasticity of substitution between air and sea transport. The disruption—driven by pandemic-related demand surges, labor shortages, and dislocations in global shipping networks, led to severe port congestion, container shortages, and sharp increases in maritime transport costs (Hu et al., 2021). These developments significantly affected global supply chains and trade flows, prompting firms to seek alternative shipping options.

Some U.S. trade routes were also affected by bilateral sanctions with Russia, particularly flights connecting the United States with Asian destinations such as Japan, China, and South Korea. Because the war in Ukraine coincided with the port disruption, I exclude 2022 from the sample to avoid confounding shocks that simultaneously affected both air and sea transport. Although the exogeneity of this episode is less clear than in the airspace closure experiment, a key advantage of this setting is the availability of direct data on transport costs by mode, product, and origin, which allows me to estimate cost responses without relying on proxies.

B.1 Empirical Strategy

I employ an empirical strategy analogous to that used for the Russian–Ukrainian conflict, comparing air and sea transport outcomes along affected and unaffected routes before and after the U.S. West Coast port disruption. Identification exploits the unexpected nature of the disruption during the post-COVID recovery period. The maintained assumption is that affected routes experienced a relative increase in maritime transport costs, while air transport costs were less directly impacted.

To document this cost differential, I use U.S. Census Bureau data reporting total transport charges for each shipment. I compute the average transport cost per kilogram for each origin–sector–time observation by dividing total transport charges by shipment weight. I then compare changes in relative transport costs by mode across treated and control groups.

The treated group consists of Asian countries that predominantly ship goods to the United States through West Coast ports.⁴¹ The control group consists of European countries, which primarily ship goods through East Coast ports that were less affected by congestion (Hu et al., 2021). As in the baseline analysis, I restrict the sample to HS6 sectors in which at least 5% of trade value was shipped by both air and sea in 2019.⁴²

I first estimate the effect of the disruption on relative transport costs:

$$\ln \left(\frac{\text{Cost}_{iht}^{\text{sea}}}{\text{Cost}_{iht}^{\text{air}}} \right) = \beta_1, \text{Disruption}_t \times \text{Treated}_i + \mu_{ih} + \mu_{th} + \epsilon_{iht}, \quad (23)$$

where $\ln (\text{Cost}_{iht}^{\text{sea}} / \text{Cost}_{iht}^{\text{air}})$ is the log ratio of average transport costs per kilogram for shipments

⁴¹In the baseline specification, treated countries include China and Hong Kong, Japan, South Korea, Taiwan, and Vietnam.

⁴²Because U.S. Census data report only air and sea shipments, land transport is not considered.

from origin country i to the United States in sector h at time t . Treated $_i$ indicates whether the origin country is affected by West Coast congestion, and μ_{ih} and μ_{th} denote origin-sector and sector-time fixed effects, respectively.⁴³ Disruption $_t$ is an indicator equal to one from January 2021 onward, following Hu et al. (2021). The coefficient β_1 captures the relative increase in maritime transport costs induced by the disruption.

I then estimate the effect of the disruption on relative trade flows by mode:

$$\ln \left(\frac{X_{iht}^{sea}}{X_{iht}^{air}} \right) = \beta_2, \text{Disruption}_t \times \text{Treated}_i + \mu_{ih} + \mu_{th} + \epsilon_{iht}, \quad (24)$$

where $\ln (X_{iht}^{sea} / X_{iht}^{air})$ is the log ratio of trade values shipped by sea relative to air. The coefficient β_2 captures the change in relative trade flows in response to the disruption. As in the baseline analysis, I compute the elasticity of substitution between air and sea transport using a Wald difference-in-differences estimator, equivalent to a two-stage least squares (2SLS) approach.

B.2 Identification Assumptions

This subsection evaluates the identifying assumptions underlying the analysis of the U.S. West Coast port disruption, following the same validation steps used for the Russian airspace closure.

First, Table E.16 shows that treated and control groups were similar in terms of trade values and transport costs prior to the shock. I use data from 2019, which predates both the port disruption and the COVID-19 pandemic. The similarity across groups reduces concerns that differential pre-shock trends or sample composition drive the results.

Second, Figure B.14 illustrates that relative maritime transport costs increased disproportionately for treated countries. The left panel shows a rightward shift in the distribution of sea transport costs for treated origins, indicating higher per-unit shipping costs from Asia. By contrast, the right panel shows relatively stable cost distributions for the control group.

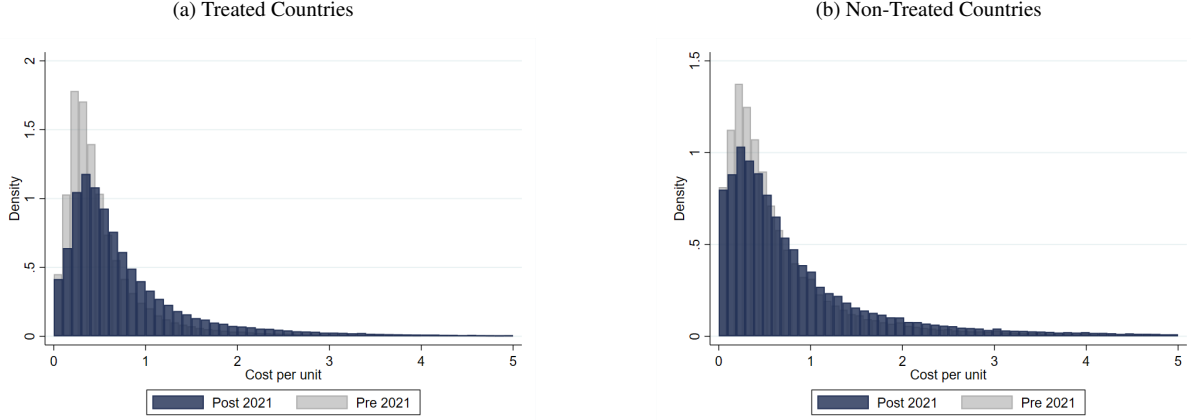
Finally, Figure B.15 presents event-study estimates based on equations (23) and (24). The left panel plots the evolution of relative transport costs, while the right panel plots relative trade flows by mode. Both panels indicate that congestion at U.S. West Coast ports led to an increase in relative maritime transport costs and a corresponding decline in sea trade for treated countries. Although the cost series exhibits greater volatility, likely reflecting noise associated with the post-COVID recovery, the absence of differential pre-trends and the alignment of cost and quantity responses support a causal interpretation of the estimates.

B.3 Results

Table B.6 reports the estimation results for equations (23) and (24). Column (1) shows a significant increase in the average transport cost per kilogram for affected countries relative to non-affected countries following the onset of the disruption. The estimated coefficient is 0.117,

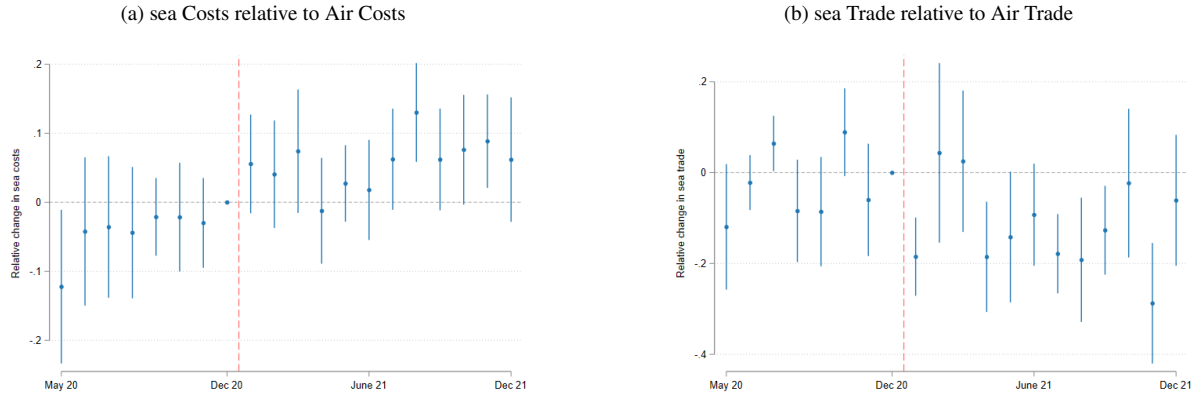
⁴³Since the Census data report only U.S. imports, the destination country is always the United States.

Figure B.14: US Data: Change in sea Transport Costs



Notes: Panel (a) shows the distribution of sea costs in the treated group before and after the shock. Panel (b) shows the same for the control group. The treated group experienced a significant increase in sea costs compared to the control group.

Figure B.15: US Data: Event Studies



Notes: Panel (a) reports the event study corresponding to equation (23), while panel (b) reports the event study corresponding to equation (24). The treated group is composed of US trading partners in Asia, while the control group is composed of European partners. We can see that after 2021 when congestion starts to engulf US West Coast ports there is a significant increase in the sea relative price in affected routes. Moreover, the relative trade flows by sea decrease significantly.

implying that average maritime transport costs increased by approximately 11 percent after the disruption.

Column (2) reports a “naive” OLS specification that directly relates monthly changes in relative freight costs to changes in relative trade shares by mode. The estimated coefficient is substantially smaller, suggesting that short-run monthly fluctuations in transport costs generate limited reallocation across modes. Instead, the larger effects captured by the difference-in-differences strategy reflect longer-run adjustments in shipping behavior in response to persistent cost shocks.

Column (3) shows that relative sea trade declined significantly compared with air trade following the disruption. Column (4) reports the implied elasticity of substitution between sea and air transport obtained using the 2SLS (Wald-DiD) strategy, which corresponds to the ratio of the coefficients in columns (3) and (1). Finally, column (5) demonstrates that the results are robust to measuring trade flows in physical quantities rather than values.

Table B.6: Substitution Between Modes of Transport: Sea to Air

	(1) $\ln(\ln Freight^{Sea}/\ln Freight^{Air})$	(2) $\ln(X^{Sea}/X^{Air})$	(3) $\ln(X^{Sea}/X^{Air})$	(4) $\ln(X^{Sea}/X^{Air})$	(5) $\ln(X^{Sea}/X^{Air})$
In Freight Ratio		-0.144 (0.003)		-1.565 (0.532)	-1.327 (0.526)
Post \times Treated	0.117 (0.030)		-0.183 (0.032)		
$\hat{\eta}$.	.	.	2.57	2.33
Obs.	1,162,343	1,162,343	1,162,343	1,162,343	1,136,097
Origin-Destination-HS6	✓	✓	✓	✓	✓
Year-Month-HS6	✓	✓	✓	✓	✓
F-Test	.	.	.	15.35	15.23
R ²	0.37	0.69	0.68	-1.40	-0.25

Notes: Column (1) reports the estimates for regression (23). The dependent variable is the log costs for an origin-HS6 sector to the US. Column (2) reports the “naive” estimator OLS results. Column (3) reports the estimates for regression (24). The dependent variable is the relative log value of trade imported from an origin-HS6 sector pair. Treated is a dummy that takes a value of 1 if the trade partner is in Asia and 0 otherwise. Disruption is a dummy that takes a value of 1 after January 2021. Column (4) reports the estimate for the equivalent 2SLS-IV estimator. Standard errors clustered at the origin-HS6 level. Column (5) reports the results for the estimation using weights ratios. Standard errors clustered at the origin-HS6 level.

This ratio can be interpreted as the effect of a 1 percent increase in transport costs, proxied by the average cost per kilogram, on the relative share of trade shipped by sea. The estimates reported in the table imply an elasticity of substitution between air and sea transport of approximately 2.57. In economic terms, a 1 percent increase in maritime transport costs leads to about a 2.6 percent increase in the share of trade shipped by air.

Comparing this estimate with the elasticity obtained in Table 1 shows that the two values are remarkably similar, despite being identified in distinct institutional settings and through different shocks. This consistency lends support to the CES assumption underlying the model, which posits a single elasticity parameter governing substitution between transport modes across contexts.

C Theory Appendix

C.1 Solution of the Discrete Choice Model

In this section, I show how to obtain the main equations of Section 3.2.2. In the first stage, the consumer chooses which good to consume, while in the second, she decides the quantity. Consider a mode $m \in M$ and denote the conditional direct utility of a consumer, in country n buying a good from country i using mode m as $u_{ni}^m = \ln q_{ni}^m$. The price that she will face is equal to $p_{ni}^m = p_i d_{ni}^m$. With p_i as the factory-gate price.

Maximizing this utility leads to demand q_{ni}^m . I can now write the indirect utility as

$$V(p_{ni}^m) = \ln p_i + \ln d_{ni}^m - \ln y_n, \quad (25)$$

where y_n is the total expenditure. In the first stage of the problem, I assume that the choice of

mode m follows the stochastic utility approach:

$$u_{ni}^m = V(p_{ni}^m) + \mu\epsilon_{ni}^m,$$

with $\mu > 0$ and ϵ_{ni}^m that follow an extreme value type I distribution (Gumbel). Since in this step the country-pair flow is already decided, I will drop the ni notation for the remaining of the subsection.

The probability density of ϵ^m is $f(\epsilon^m) = \exp(-\epsilon^m) \exp(-\exp(-\epsilon^m))$. The cumulative density function is $F(\epsilon^m) = \exp(-\exp(-\epsilon^m))$. The probability of choosing mode m instead of mode k is:

$$\begin{aligned} Pr(u^m > u^k) &= Pr(V^m + \mu\epsilon^m > V^k + \mu\epsilon^k) \\ &= Pr(V^m - V^k + \mu\epsilon^m > \mu\epsilon^k). \end{aligned}$$

While the conditional probability is

$$Pr(u^m > u^k | \epsilon^m) = F(V^m - V^k + \mu\epsilon^m),$$

and the conditional probability of choosing m given the other options is:

$$Pr(u^m > u^k \forall k \neq m | \epsilon^m) = \prod F(V^m - V^k + \mu\epsilon^m).$$

Finally, the unconditional probability of the mode m is given by

$$Pr(u^m > u^k \forall k \neq m) = \int_{-\infty}^{\infty} \prod_{k \neq m} F(V^m - V^k + \mu\epsilon^m) f(\epsilon^m) d\epsilon^m.$$

Now we have to substitute in the definitions of $F(\cdot)$ and $f(\cdot)$ and solve

$$\begin{aligned} Pr^m &= \int_{-\infty}^{\infty} \prod_{k \neq m} F(V^m - V^k + \mu\epsilon^m) f(\mu\epsilon^m) d\epsilon^m \\ &= \int_{-\infty}^{\infty} \prod_{k \neq m} \exp(-\exp(V^m - V^k + \mu\epsilon^m)) \exp(-\mu\epsilon^m) \exp(-\exp(-\mu\epsilon^m)) d\epsilon^m \\ &= \int_{-\infty}^{\infty} \prod_k \exp(-\exp(V^m - V^k + \mu\epsilon^m)) \exp(-\mu\epsilon^m) d\epsilon^m \\ &= \int_{-\infty}^{\infty} \exp(-\exp(-\mu\epsilon^m)) \sum_k \exp(V^m - V^k) (-\exp(-\mu\epsilon^m)) d\epsilon^m. \end{aligned}$$

Change of variable to $t = -\exp(-\mu\epsilon^m)$ and $(1/\mu)dt = \exp(-\mu\epsilon^m)$.

$$Pr^m = \int_{-\infty}^0 \exp(t \sum_k \exp(V^m - V^k)) \frac{1}{\mu} dt.$$

We can now solve the integral to obtain:

$$Pr^m = \frac{1}{\sum_k \exp \left(- \left(\frac{V^m}{\mu} - \frac{V^k}{\mu} \right) \right)} = \frac{\exp \left(\frac{V^m}{\mu} \right)}{\sum_k \exp \left(\frac{V^k}{\mu} \right)}, \quad (26)$$

I can substitute equation (25) into equation (26) to have that

$$\begin{aligned} Pr^m &= \frac{\exp(V_{ni}^m/\mu)}{\sum_k \exp(V_{ni}^k/\mu)} \\ &= \frac{\exp(-\ln p_{ni}^m/\mu) \exp(-\ln y/\mu)}{\sum_k \exp(-\ln p_{ni}^k/\mu) \exp(-\ln y/\mu)} \\ &= \frac{(p_{ni}^m)^{-1/\mu}}{\sum_k (p_{ni}^k)^{-1/\mu}} \\ &= \frac{(p_i d_{ni}^m)^{-1/\mu}}{\sum_k (p_i d_{ni}^k)^{-1/\mu}} \\ \pi_{ni}^m &= \frac{(d_{ni}^m)^{-1/\mu}}{\sum_k (d_{ni}^k)^{-1/\mu}}. \end{aligned} \quad (27)$$

The share imported by destination n from origin i by mode m depends entirely on the relative costs that are specific to the modes. Since factory-gate prices and other pair-wise costs are constant across transport modes, they do not matter in determining the share. Define now the elasticity of substitution between modes of transport as $\eta = (\mu + 1)/\mu$ so that we can rewrite equation (27) as:

$$\pi_{ni}^m = \frac{(d_{ni}^m)^{1-\eta}}{\sum_k (d_{ni}^k)^{1-\eta}} = \frac{X_{ni}^m}{X_{ni}}, \quad (28)$$

where the assumption of $\mu > 0$ implies $\eta > 1$.

The share in equation (28) can be derived from a CES utility function:

$$u_{ni} = \left(\sum_{m=1}^M (q_{ni}^m)^{(\eta-1)/\eta} \right)^{\eta/(\eta-1)}, \quad (29)$$

that is maximised under the budget constraint: $\sum^M q_{ni}^m p_{ni}^m = \sum^M X_{ni}^m = X_{ni}$. Where q_{ni}^m is the quantity imported by n from i by each mode, and X_{ni} is the total value imported.

C.2 Share by mode with Congestion

The price index from the discrete random choice mode, which corresponds to the transport costs index in the upper nest, is now given by:

$$d_{ni} = \left(\sum_{m=1}^M (d_{ni}^m)^{1-\eta} \right)^{1/(1-\eta)} = \left(\sum_{m=1}^M (\delta_{ni}^m)^{1-\eta} (\Xi_{ni}^m)^{1-\eta} \right)^{1/(1-\eta)}, \quad (30)$$

and accordingly, now the share of mode s between importer i and exporter j is given by:

$$\pi_{ni}^m = \frac{(d_{ni}^s)^{1-\eta}}{\sum_{m=1}^M (d_{ni}^m)^{1-\eta}} = \frac{(\delta_{ni}^s)^{1-\eta} (\Xi_{ni}^s)^{1-\eta}}{\sum_{m=1}^M (\delta_{ni}^m)^{1-\eta} (\Xi_{ni}^m)^{1-\eta}}. \quad (31)$$

C.3 Derivation of \hat{d}_{ni} with Congestion

To derive equation (14), assume that the shock is a change in costs for mode $s \in M$ we have that

$$\begin{aligned} \hat{d}_{ni} &= d'_{ni}/d_{ni} = \frac{\left(\sum_{m=1}^M (d'_{ni}^m)^{1-\eta} (\Xi'_{ni}^m)^{1-\eta} \right)^{1/(1-\eta)}}{\left(\sum_{m=1}^M (d_{ni}^m)^{1-\eta} (\Xi_{ni}^m)^{1-\eta} \right)^{1/(1-\eta)}} \\ &= \left(\frac{(d'_{ni}^s)^{1-\eta} (\Xi'_{ni}^s)^{1-\eta} + \sum_{m \neq s} (d_{ni}^m)^{1-\eta} (\Xi_{ni}^m)^{1-\eta} \pm \sum_{m=1}^M (d_{ni}^m)^{1-\eta} (\Xi_{ni}^m)^{1-\eta}}{\sum_{m=1}^M (d_{ni}^m)^{1-\eta} (\Xi_{ni}^m)^{1-\eta}} \right)^{1/(1-\eta)} \\ &= \left(1 + \frac{(d'_{ni}^s)^{1-\eta} (\Xi'_{ni}^s)^{1-\eta} - (d_{ni}^s)^{1-\eta} (\Xi_{ni}^s)^{1-\eta}}{\sum_{m=1}^M (d_{ni}^m)^{1-\eta} (\Xi_{ni}^m)^{1-\eta}} + \frac{\sum_{m \neq s} (d_{ni}^m)^{1-\eta} (\Xi_{ni}^m)^{1-\eta} - \sum_{m \neq s} (d_{ni}^m)^{1-\eta} (\Xi_{ni}^m)^{1-\eta}}{\sum_{m=1}^M (d_{ni}^m)^{1-\eta} (\Xi_{ni}^m)^{1-\eta}} \right)^{1/(1-\eta)} \\ &= \left(1 + \frac{\left[(\hat{d}_{ni}^s)^{1-\eta} (\hat{\Xi}_{ni}^s)^{(1-\eta)} - 1 \right] (d_{ni}^s)^{1-\eta} (\Xi_{ni}^s)^{(1-\eta)}}{\sum_{m=1}^M (d_{ni}^m)^{1-\eta} (\Xi_{ni}^m)^{1-\eta}} + \frac{\sum_{m \neq s} (d_{ni}^m)^{1-\eta} (\Xi_{ni}^m)^{(1-\eta)} \left[(\hat{\Xi}_{ni}^m)^{(1-\eta)} \right]}{\sum_{m=1}^M (d_{ni}^m)^{1-\eta} (\Xi_{ni}^m)^{1-\eta}} \right)^{1/(1-\eta)} \\ &= \left[1 + \left((\hat{d}_{ni}^s (\hat{X}_{ni}^s)^\lambda)^{1-\eta} - 1 \right) \pi_{ni}^s + \sum_{m \neq s} \pi_{ni}^m \left((\hat{X}_{ni}^m)^{(\lambda)(1-\eta)} - 1 \right) \right]^{1/(1-\eta)} \end{aligned}$$

where in the last step I use the definition of the share of mode m in equation (31) and the fact that $\hat{\Xi}_{ni}^s = (\hat{X}_{ni}^s)^\lambda$, since infrastructures are assumed to be constant.

C.4 Interpretation of η with Congestion

Since congestion affects the ability of agents to substitute it can also affect the interpretation of the parameter estimated in the previous section. Within this framework, I show that the share of each mode can be determined using equation (31). As a consequence, congestion costs could change the interpretation of the elasticity parameter, η , recovered in the previous section using equation (4).

However, the distortion introduced by congestion costs will downward bias the elasticity of substitution between modes. In fact, the congestion costs will make the mode that is used more expensive and, therefore, less utilized, while the other modes will be used more. This will lead to a lower elasticity of substitution between modes. It is also possible to demonstrate this analytically by taking the ratio of equation (31) between two generic transport modes m and s by bringing the flows by transport mode to the right-hand side:

$$\ln \left(\frac{X_{ni}^m}{X_{ni}^s} \right) = \frac{1-\eta}{1-\lambda(1-\eta)} \ln \left(\frac{d_{ni}^m}{d_{ni}^s} \right),$$

moreover, we can see that for values of λ close to zero the bias will disappear. Since a value approaching zero for the congestion parameter is usually found in the literature ([Allen and Arkolakis, 2022](#); [Fuchs and Wong, 2024](#)) I believe that the parameter identified is a good approximation of the true elasticity of substitution or at least a lower bound.

Using the estimated values, β_{did} , from the previous section and the congestion strength $\lambda = 0.079$ estimated in the main text, we obtain values for the elasticity of substitution between modes, once congestion is taken into account, of $\eta \approx 2.83$. ⁴⁴

C.5 Model with Cobb-Douglas Shares

With Cobb-Douglas share by mode, the transportation costs index is given by the following:

$$d_{ni} = \prod_{m=1}^M (d_{ni}^m)^{\pi_{ni}^m}$$

Since shares are constant and the change in costs affects only one mode, the counterfactual change in the aggregate trade costs is given by

$$\hat{d}_{ni} = (\hat{d}_{ni}^s)^{\pi_{ni}^s}$$

where s is the mode shocked and the share π is constant. Note that the equations for the rest of the system in changes remain unchanged by this new definition of trade costs.

C.6 Model with Cobb-Douglas Shares and Congestion

With Cobb-Douglas share by mode and congestion as described in Section 6, the transportation costs index is given by the following:

$$d_{ni} = \prod_{m=1}^M (d_{ni}^m)^{\pi_{ni}^m} = \prod_{m=1}^M (\delta_{ni}^m \Xi_{ni}^m)^{\pi_{ni}^m}$$

Since shares are constant and the change in costs affects only one mode, the counterfactual change in the aggregate trade costs is given by

$$\hat{d}_{ni} = \left(\hat{\delta}_{ni}^s \left(\hat{X}_{ni}^s \right)^\lambda \right)^{\pi_{ni}^s} \prod_{m \neq s} \left(\left(\hat{X}_{ni}^m \right)^\lambda \right)^{\pi_{ni}^m}$$

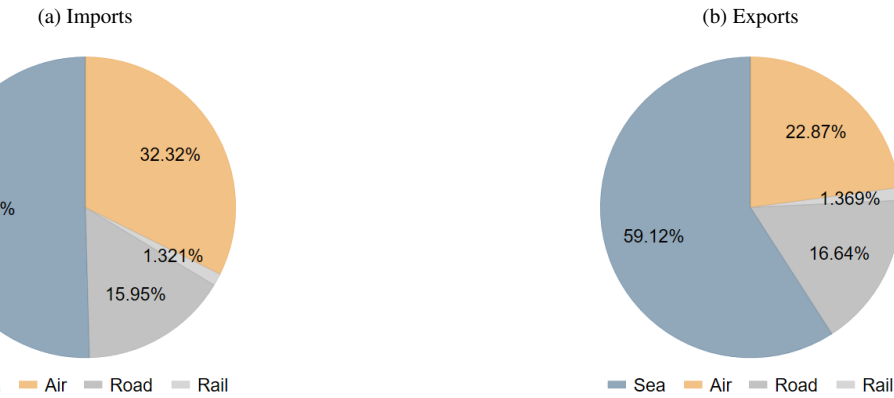
where s is the mode shocked and the share π is constant. As for the previous case, the rest of the system is equal to the baseline case.

⁴⁴To see this just solve for:

$$\hat{\beta}_{Did} = \frac{1 - \eta}{1 - \lambda(1 - \eta)} \quad \rightarrow \quad \eta = 1 - \frac{\hat{\beta}_{Did}}{1 + \hat{\beta}_{Did}\lambda}$$

D Additional Figures

Figure D.1: Transport Mode Share of Trade



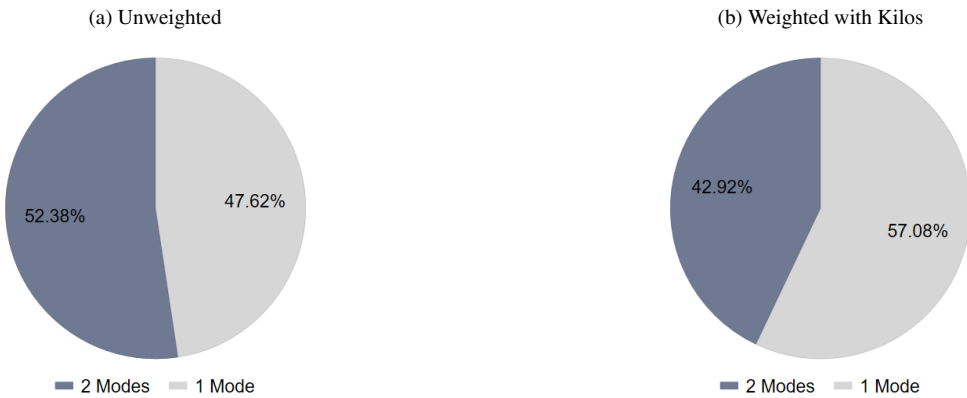
Notes: Panel (a) reports the aggregate share of imported trade in euros by mode of transport. Panel (b) reports the aggregate share of exported trade in euros by mode of transport. The sample consists of European Union members' trade flows in euros in 2019, collected from Eurostat.

Figure D.2: Transport Mode Share of Trade



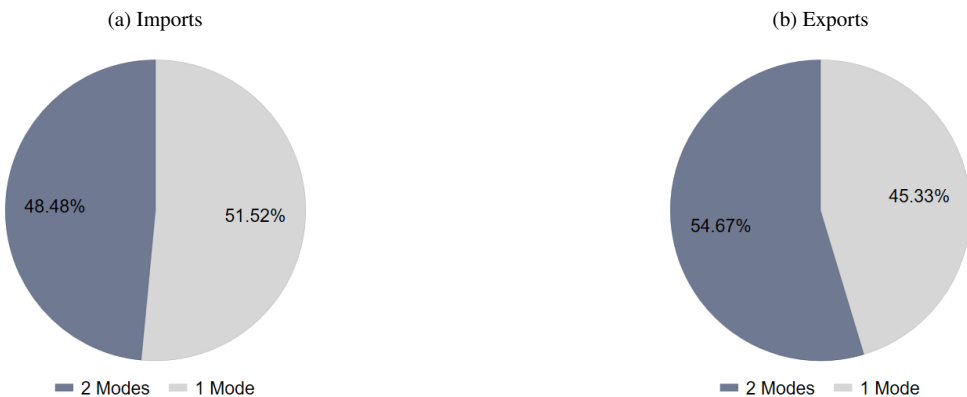
Notes: Panel (a) reports the aggregate share of trade in euros by mode of transport with the United States. Panel (b) reports the aggregate share of trade in euros by mode of transport with China. The sample consists of European Union members' trade flows in euros in 2019, collected from Eurostat.

Figure D.3: Number of Modes Used per Origin-Destination-HS6: Alternative



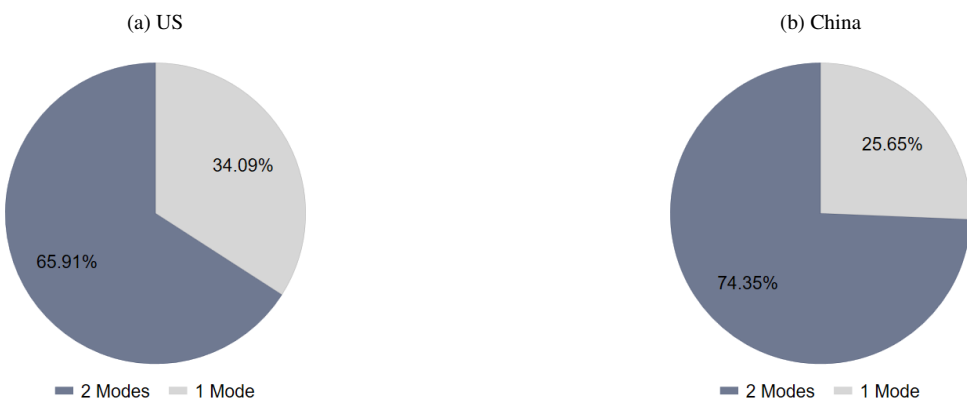
Notes: Panel (a) shows the percentage of origin-destination-HS6 sectors that use both air and ocean transport unweighted. Panel (b) shows the percentage of origin-destination-HS6 sectors that use both air and ocean transport weighted with kilos. The sample consists of imports and exports of European Union members in 2019, collected from Eurostat.

Figure D.4: Number of Modes Used per Origin-Destination-HS6: Imports vs Exports



Notes: Panel (a) shows the percentage of origin-destination-HS6 sectors that use both air and ocean transport for imports. Panel (b) shows the percentage of origin-destination-HS6 sectors that use both air and ocean transport for exports. The sample consists of imports and exports of European Union members in 2019, collected from Eurostat.

Figure D.5: Number of Modes Used per Origin-Destination-HS6: US vs China



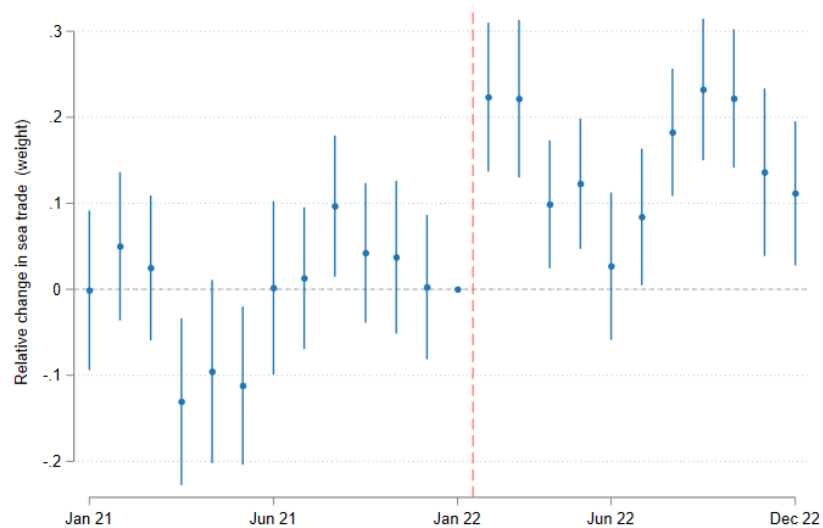
Notes: Panel (a) shows the percentage of origin-destination-HS6 sectors that use both air and ocean transport from the United States. Panel (b) shows the percentage of origin-destination-HS6 sectors that use both air and ocean transport from China. The sample consists of imports and exports of European Union members in 2019, collected from Eurostat.

Figure D.6: Flight Path Cargo vs Passenger



Notes: Flight route between Frankfurt and Beijing after the start of the Ukraine war for a passenger flight vs a cargo flight. Author's own calculation based on Flightradar24 data.

Figure D.7: Flight Path Cargo vs Passenger



Notes: This figure reports the event study based on equation (17) and shows that there is a significant increase in sea trade, in kilograms, relative to air trade after the closure of the Russian and Ukrainian airspace between treated and non-treated country pairs.

E Additional Tables

Table E.7: Comparison of Treated and Control Groups

	Group	Mean	Median	Std. Dev.
<i>Panel A. Air Trade</i>				
Log weight	Non-treated	8.39	8.56	2.26
	Treated	8.73	9.00	2.54
Log value	Non-treated	12.66	12.83	2.64
	Treated	12.64	12.87	2.77
<i>Panel B. Sea Trade</i>				
Log weight	Non-treated	9.35	9.75	3.25
	Treated	10.49	10.97	3.15
Log value	Non-treated	12.35	12.76	2.99
	Treated	13.21	13.58	1.78

Notes: The table compares treated and control groups to assess whether the estimated effects are driven by pre-shock differences in trade composition. The treated group consists of country pairs formed by European countries and destinations in Eastern or Southern Asia. The control group includes all other country pairs. Data are from Eurostat for 2019. The unit of observation is monthly bilateral trade flows at the country-pair-sector level. Sectors are defined at the HS6 level.

Table E.8: Air Trade and Product Characteristics

	% with two modes	Value by air (%)	Weight by air (%)	Observations
<i>Panel A. Broad Economic Classification (BEC)</i>				
Other (0)	35.95	0.021	0.005	7,710
Capital (1)	53.79	0.390	0.060	377,449
Intermediate (2)	54.38	0.271	0.004	1,209,396
Consumption (3)	49.30	0.274	0.025	627,600
<i>Panel B. Containerizability</i>				
Not suitable (0)	52.99	0.054	0.001	193,513
Slightly suitable (1)	44.35	0.202	0.010	151,770
Suitable (2)	53.44	0.347	0.018	1,876,892
<i>Panel C. Temperature Sensitivity</i>				
Low (1)	53.61	0.242	0.005	1,488,940
Medium–Low (2)	54.63	0.285	0.006	433,532
Medium–High (3)	48.78	0.515	0.015	178,331
High (4)	41.85	0.332	0.024	121,372
<i>Panel D. Unit Value</i>				
Low (1)	46.41	0.014	0.002	424,815
Medium (2)	57.46	0.103	0.025	785,724
High (3)	51.83	0.445	0.098	1,011,604
<i>Panel E. Time Costs</i>				
Low (1)	47.56	0.405	0.011	653,082
Medium (2)	54.17	0.326	0.027	814,913
High (3)	55.80	0.085	0.003	754,180

Notes: This table reports descriptive statistics for Eurostat trade flows by product characteristics. The Broad Economic Classification (BEC) categorizes products by final use. Containerizability measures the ease with which a good can be transported in containers (from Bernhofen et al., 2016). Temperature sensitivity is an index ranging from 1 (low) to 4 (high). Unit value is defined as terciles of the sector-level unit value distribution in 2019. Time costs are based on a discretized version of the continuous index in Hummels and Schaur (2013).

Table E.9: Elasticity by ISIC3 sector

Sector	lnftime	(SE)	Obs.	K-P F-stat	1st stage	Mean DV	Origin-Destination-HS6	Year-Month-HS6
Agriculture	1.242	(1.830)	10,392	34.65	0.063	0.59	✓	✓
Auto	4.127	(1.198)	13,247	88.10	0.096	0.60	✓	✓
Basic Metals	1.734	(0.793)	61,363	253.80	0.067	0.68	✓	✓
Chemicals	1.834	(0.474)	182,206	742.94	0.062	0.87	✓	✓
Communication	2.308	(0.877)	58,484	283.02	0.072	-0.40	✓	✓
Electrical	0.864	(0.348)	245,669	1297.11	0.077	-0.07	✓	✓
Food	1.023	(1.509)	17,227	66.39	0.059	1.53	✓	✓
Machinery n.e.c	0.594	(0.213)	458,308	2502.85	0.081	0.42	✓	✓
Manufacturing n.e.c	3.082	(0.690)	78,728	302.70	0.072	0.56	✓	✓
Medical	1.354	(0.423)	175,488	834.35	0.075	-0.79	✓	✓
Metal Products	0.575	(0.333)	227,257	1062.81	0.074	0.26	✓	✓
Minerals	2.201	(0.705)	57,572	243.74	0.074	0.70	✓	✓
Mining	289.214	(19095.535)	316	0.00	-0.001	0.56	✓	✓
Misc	7.708	(7.933)	717	3.48	0.050	1.32	✓	✓
Office	0.222	(1.234)	26,295	113.55	0.070	-1.30	✓	✓
Other Business	31.833	(75.583)	194	0.74	-0.013	-1.28	✓	✓
Other Transport	-4.480	(8.545)	5,545	2.98	0.037	-0.80	✓	✓
Paper	-0.287	(0.736)	53,453	238.91	0.071	-0.09	✓	✓
Plastic	1.847	(0.544)	77,367	422.02	0.080	0.63	✓	✓
Textile	3.584	(0.419)	292,813	770.50	0.059	0.00	✓	✓
Wood	2.012	(1.823)	9,549	51.71	0.066	1.07	✓	✓

Notes: This table reports the results of the estimation of equation (18) by ISIC3 sectors. All estimates include origin-destination-hs6 and year-month-hs6 fixed effect. Standard errors are clustered at the origin-destination-hs6 level. All the estimations are performed via OLS.

Table E.10: Elasticity by Product Characteristics

Sample		lnftime	(s.e.)	Obs.	Origin-Destination-HS6	Year-Month-HS6	F-Test
BEC	Capital	1.046	(0.638)	526,758	✓	✓	25.95
	Intermediate	1.468	(0.523)	1,633,209	✓	✓	27.75
	Consumption	2.660	(1.172)	608,364	✓	✓	11.06
Containerization	No Suitable	0.810	(0.413)	224,487	✓	✓	39.26
	Slightly Suitable	4.058	(1.539)	118,457	✓	✓	9.53
	Suitable	1.600	(0.614)	2,425,728	✓	✓	22.65
Temperature Sensitivity	Low	1.480	(0.576)	1,884,728	✓	✓	22.38
	Mid-low	2.048	(0.653)	567,606	✓	✓	24.99
	Mid-high	1.359	(0.808)	247,994	✓	✓	23.40
	High	2.105	(0.966)	68,344	✓	✓	24.50
Time Cost	Low	2.050	(1.042)	413,731	✓	✓	13.17
	Mid	1.534	(0.646)	834,322	✓	✓	23.32
	High	1.742	(0.563)	641,868	✓	✓	22.87
	Very High	1.367	(0.503)	878,751	✓	✓	28.74

Notes: This table reports the results of the estimation of equation (18) by product characteristics. The Broad Economic Classification (BEC) is an indicator variable that categorizes products based on their final use and is composed of three main categories: Capital, Intermediate, and Consumption goods. Containerizability is an index that describes how easy it is for a good to be transported in a container. This measure is taken from Bernhofen et al. (2016). Temperature is an index that measures how sensitive a good is to temperature, and it takes values from 1 (low sensitivity) to 4 (high sensitivity). The time costs index is a discretized version of the continuous index by Hummels and Schaur (2013). All estimates include origin-destination-hs6 and year-month-hs6 fixed effect. Standard errors are clustered at the origin-destination-hs6 level. All the estimations are performed via OLS.

Table E.11: Substitution Between Modes of Transport: Weight

	(1) ln FlightTime	(2) ln (X^{Sea}/X^{Air})	(3) ln (X^{Sea}/X^{Air})	(4) ln (X^{Sea}/X^{Air})
In FlightTime			1.895 (0.611)	2.267 (0.785)
Post × Treated	0.071 (0.015)	0.134 (0.030)		
In Freight				0.039 (0.023)
$\hat{\eta}$			3	3.27
Obs.	2,822,346	2,822,346	2,822,346	2,822,346
Origin-Destination-HS6	✓	✓	✓	✓
Year-Month-HS6	✓	✓	✓	✓
F-Test			23.15	18.39
R ²	0.85	0.59	-0.01	-0.02

Notes: Column (1) reports the estimates for regression (16). The dependent variable is the log average flight time between two country pairs. Column (2) reports the estimates for regression (17) where the dependent variable is the ratio, in euros, between sea and air trade between a country n and a country i in sector h in month t . Treated is a dummy that takes values 1 if the origin/destination country is in Asia and 0 otherwise. Post is a dummy that takes value 1 after the start of the war (February 2022) and 0 otherwise. The Wald-DiD estimator, equation (18), is calculated via 2SLS and is equivalent to the ratio of the coefficients in columns (1) and columns (2). The coefficient of column (3) can be interpreted as the elasticity of substitution between transport modes. Standard errors are clustered at the origin-destination-year level. Column (4) includes freight indexes from major European Ports to Asian and American destinations.

Table E.12: Substitution Between Modes of Transport:: UV ratio

	(1) Low	(2) Med-low	(3) Med-High	(4) High
lnftime	2.533 (1.120)	1.807 (0.709)	1.805 (0.585)	1.051 (0.497)
$\hat{\eta}$	3.53	2.81	2.80	2.05
Obs.	282,204	675,478	924,758	939,399
Origin-Destination-HS6	✓	✓	✓	✓
Year-Month-HS6	✓	✓	✓	✓
F-Test	11.43	20.25	25.48	27.67

Notes: The dependent variable is the log average flight time between two country pairs. The sample is divided based on the ratio of the unit values by mode within an origin-destination-sector. Standard errors are clustered at the origin-destination-year level.

Table E.13: Substitution Between Modes of Transport: Robustness

	(1) Full Sample	(2) Manufacture	(3) March 22	(4) Alt Cluster	(5) Alt Cluster 2	(6) No Landlock
In FlightTime	1.331 (0.583)	1.530 (0.589)	1.220 (0.456)	1.594 (0.107)	1.594 (0.701)	1.593 (0.615)
$\hat{\eta}$	2.33	2.53	2.22	2.59	2.59	2.59
Obs.	2,187,907	2,592,594	2,768,672	2,768,672	2,768,672	2,679,633
Origin-Destination-HS6	✓	✓	✓	✓	✓	✓
Year-Month-HS6	✓	✓	✓	✓	✓	✓
F-Test	24.75	23.52	24.88	11,997.55	17.33	21.44

Notes: Column (1) reports estimates using the full sample, Column (2) restricts the sample to manufacturing sectors, Column (3) defines the start of the sanctions period as March 2022. Column (4) reports estimates using standard errors clustered at the origin–destination–HS6 level, Column (5) reports estimates using standard errors clustered at the origin–destination level. Column (6) excludes European countries that are landlocked (Austria, Czech Republic, Hungary, and Slovakia). Standard errors are clustered at the origin-destination-year level.

Table E.14: Impact on Within Product Composition

	(1) UV Ratio	(2) UV Air	(3) UV Sea
In FlightTime	0.195 (0.221)	0.195 (0.233)	-0.000 (0.222)
Obs.	3,069,425	3,069,425	3,069,425
Origin-Destination-HS6	✓	✓	✓
Year-Month-HS6	✓	✓	✓
F-Test	23.72	17.64	17.64

Notes: This table reports the estimates for the Wald-Did estimator computed via IV-2SLS by unit values calculated at the origin-destination-sector-transport level. Column (1) reports the results for the ratio between air and sea unit values within a common origin-destination-sector triplet. Columns (2) and (3) instead estimate the effect separately. Standard errors are clustered at the origin-destination level.

Table E.15: Substitution Between Modes of Transport: Naive OLS

	(1) $\ln(X^{Sea}/X^{Air})$	(2) $\ln(X^{Sea}/X^{Air})$
In FlightTime	-0.054 (0.050)	-0.042 (0.048)
Obs.	2,821,847	2,753,888
Origin-Destination-HS6	✓	✓
Year-Month-HS6	✓	✓
R^2	0.61	0.58

Notes: This table reports the estimates for “naive” OLS in which I regress changes in the relative trade share by mode on flight time. Standard errors are clustered at the origin-destination level.

Table E.16: Comparison of Treated and Control Groups: U.S. Census Data

	Group	Mean	Median	Std. Dev.
<i>Panel A. Air Trade</i>				
Log value	Non-treated	11.48	11.41	2.26
	Treated	11.86	11.85	1.45
Log cost	Non-treated	1.19	1.29	1.25
	Treated	1.34	1.50	1.22
<i>Panel B. Sea Trade</i>				
Log value	Non-treated	12.07	12.15	2.28
	Treated	13.53	13.68	2.44
Log cost	Non-treated	-0.67	-0.59	1.47
	Treated	-0.63	-0.60	1.17

Notes: The table compares treated and control groups to assess whether the estimated effects are driven by pre-shock differences in trade composition. The treated group consists of U.S. trading partners in Asia, while the control group includes European partners. The unit of observation is monthly bilateral trade flows by transport mode at the country-pair-sector level. Sectors are defined at the HS6 level. Data refer to 2019, prior to the shock and the COVID-19 pandemic.

Table E.17: Congestion and Transport Costs: EU Shift

	(1) $\ln freight_{omkt}$ IV	(2) $\ln freight_{omkt}$ IV Air	(3) $\ln freight_{omkt}$ IV Sea
Log Weight	0.089 (0.009)	0.108 (0.013)	0.066 (0.011)
Obs.	636,249	344,240	290,827
Origin-Year-HS4-Mode	✓		
Origin-Year-HS4		✓	✓
Year-Month-Origin	✓	✓	✓
First Stage	0.43	0.40	0.44
F-Test	1,681.04	1,548.57	809.19

Notes: Column (1) reports the results of the OLS estimation for equation (19). Columns (2) to (4) instead report the Shift-share Iv strategy. The sample used consist of US imports from 2014 to 2019 at the monthly frequency from the US Census Bureau. The shift is calculated using EU exports to non-US destinations in the same period. Standard errors in parenthesis are clustered at the origin level.

Table E.18: Congestion and Transport Costs: Alternative Fixed Effects

	(1) Log Freight Cost IV	(2) Log Freight Cost IV Air	(3) Log Freight Cost IV Sea	(4) Log Freight Cost IV	(5) Log Freight Cost IV Air	(6) Log Freight Cost IV Sea
Log Weight	0.110 (0.010)	0.126 (0.016)	0.098 (0.013)	0.113 (0.010)	0.176 (0.025)	0.098 (0.015)
Obs.	621,569	335,332	285,095	633,421	339,831	284,888
Origin-Quarter-HS4-Mode	✓					
Origin-Quarter-HS4		✓	✓			
Origin-Year-HS4-Mode				✓		
Origin-Year-HS4					✓	✓
Year-Month-Origin	✓	✓	✓	✓	✓	✓
Year-Month-HS4				✓	✓	✓
First Stage	0.44	0.39	0.47	0.43	0.37	0.47
F-Test	1,143.67	797.87	862.69	697.71	218.45	709.22

Notes: Columns (1)-(3) reports the results of the estimation for equation (19) using origin-product-quarter fixed effects. Columns (4) to (6) instead report the estimate including an year-month-fixed effect. The sample used consist of US imports from 2014 to 2019 at the monthly frequency from the US Census Bureau. Standard errors in parenthesis are clustered at the origin level.

Table E.19: Congestion and Transport Costs: Alternative Samples

	(1) Log Freight Cost IV	(2) Log Freight Cost IV Air	(3) Log Freight Cost IV Sea	(4) Log Freight Cost IV	(5) Log Freight Cost IV Air	(6) Log Freight Cost IV Sea
Log Weight	0.086 (0.008)	0.102 (0.010)	0.079 (0.011)	0.029 (0.006)	0.037 (0.010)	0.022 (0.007)
Obs.	948,925	513,171	434,036	2,613,144	1,229,503	1,381,124
Sample	2014-2022	2014-2022	2014-2022	All	All	All
Origin-Year-HS4-Mode	✓			✓		
Origin-Year-HS4		✓	✓		✓	✓
Year-Month-Origin	✓	✓	✓	✓	✓	✓
First Stage	0.43	0.38	0.45	0.31	0.26	0.34
F-Test	1,898.86	1,123.57	1,501.16	1,376.20	937.69	1,365.08
R ²	-0.06	-0.08	-0.04	-0.02	-0.03	-0.01

Notes: Columns (1)-(3) reports the results of the estimation for equation (19) using years 2019-2022. Columns (4) to (6) instead report the estimate including an also 2012 and 2014. The sample used consist of US imports at the monthly frequency from the US Census Bureau. Standard errors in parenthesis are clustered at the origin level.

Table E.20: Data Sources and Parameters for Counterfactual Analysis

Variable	Source	Currency	Exchange rate	Classification	Year
<i>Panel A. Trade Shares by Mode</i>					
Extra-European trade	Eurostat	EUR	1.1069 (ECB)	HS6	2018
Japan	Trade Statistics of Japan	JPY	108.79 (IMF)	CN8	2018
United States	U.S. Census Bureau	USD		CN8	2018
Latin America	IDB Database	USD		CN8	2018
ASEAN countries	ASEAN Database	USD		CN8	2021
Other countries	Comtrade	USD		HS6	2018
China	Imputed				2018
Rest of the world	Imputed				2018
<i>Panel B. Trade Flows</i>					
International trade	Comtrade	USD		HS6	2018
Intra-country trade	TradeProd (CEPII)	USD		ISIC Rev. 3	2018
<i>Panel C. Country-Level Statistics</i>					
GDP	World Bank	USD			2018
PPP	World Bank	USD			2018
Balance of payments	IMF	USD			2018
<i>Panel D. Structural Parameters</i>					
α	Eaton and Kortum (2002)	0.188			
β	Eaton and Kortum (2002)	0.312			
θ	Head and Mayer (2014)	4			
λ_{air}	Own calculation	0.097			
λ_{sea}	Own calculation	0.060			
η	Own calculation	2.6			

Notes: Unless otherwise stated, data refer to 2018. Trade shares by mode for Latin American countries are based on 2018 data, while those for ASEAN countries are based on 2021 data due to data availability. Trade flows are converted to ISIC Rev. 3 to ensure comparability with intra-country trade flows. The Latin American sample includes Brazil, Chile, Colombia, Costa Rica, the Dominican Republic, Ecuador, Jamaica, Mexico, Peru, and Uruguay. The ASEAN sample includes Brunei, Cambodia, Indonesia, Malaysia, Myanmar, the Philippines, Singapore, Thailand, and Viet Nam. The group of other countries includes Australia, Benin, Bosnia, Belize, Canada, Côte d'Ivoire, Madagascar, Mauritius, Nigeria, El Salvador, Türkiye, and South Africa. Following the TradeProd dataset, only sectors related to industrial production are retained. The HS2 sectors used (in parentheses) are: *Chemicals* (23–25), *Food* (15–16), *Machinery* (29–33), *Metals* (27–28), *Minerals* (26), *Other* (36), *Textiles* (17–19), *Vehicles* (34–35), and *Wood and paper* (20–22). Chinese trade flows by transport mode are inferred from other flows and converted accordingly. Intra-country trade flows are not reported by transport mode. Trade by mode is restricted to air and sea, which together account for more than 90% of total observed trade.

Table E.21: List of Countries Used

ISO code	Country name	ISO code	Country name
AUS	Australia	ITA	Italy
AUT	Austria	JAM	Jamaica
BEL	Belgium	JPN	Japan
BEN	Benin	LTU	Lithuania
BGR	Bulgaria	LUX	Luxembourg
BLZ	Belize	LVA	Latvia
BRA	Brazil	MDG	Madagascar
BRN	Brunei Darussalam	MEX	Mexico
CAN	Canada	MMR	Myanmar
CHL	Chile	MUS	Mauritius
CHN	China	MYS	Malaysia
CIV	Côte d'Ivoire	NGA	Nigeria
COL	Colombia	NLD	Netherlands
CRI	Costa Rica	PER	Peru
CYP	Cyprus	PHL	Philippines
CZE	Czechia	POL	Poland
DEU	Germany	PRT	Portugal
DNK	Denmark	ROU	Romania
DOM	Dominican Republic	SGP	Singapore
ECU	Ecuador	SLV	El Salvador
ESP	Spain	SVK	Slovakia
EST	Estonia	SWE	Sweden
FIN	Finland	THA	Thailand
FRA	France	TUR	Türkiye
GBR	United Kingdom	URY	Uruguay
GRC	Greece	USA	United States of America
HUN	Hungary	VNM	Viet Nam
IDN	Indonesia	ZAF	South Africa
IRL	Ireland	ROW	Rest of the world

Table E.22: Welfare and Emissions Effects of Airspace Closure

Country	Change in relative shares	Welfare change	Δ welfare	CO ₂ imports
Australia	0.000	-0.003		0.074
Benin	0.000	-0.013		
Belize	0.000	0.009		
Brazil	0.000	0.000		0.191
Brunei Darussalam	0.000	0.014		0.215
Canada	0.000	-0.001		0.081
Chile	0.000	0.001		0.111
China	-0.100	-0.025	7.347	-0.481
Côte d'Ivoire	0.000	0.002		0.464
Colombia	0.000	-0.002		0.123
Costa Rica	0.000	0.005		
Dominican Republic	0.000	-0.005		-0.012
Ecuador	0.000	0.001		0.073
Europe	-0.099	-0.120	5.526	-0.058
Indonesia	-0.099	-0.016	0.441	-0.118
Jamaica	0.000	-0.006		0.016
Japan	-0.101	-0.050	4.858	-0.128
Madagascar	0.000	0.011		0.085
Mexico	0.000	0.006		0.147
Myanmar	-0.100	-0.016	2.003	-0.155
Mauritius	0.000	0.001		
Malaysia	-0.101	-0.099	4.131	-0.357
Nigeria	0.000	-0.002		0.433
Peru	0.000	0.001		0.128
Philippines	-0.101	-0.089	6.403	-0.587
Singapore	-0.101	-0.282	2.374	-0.419
Thailand	-0.101	-0.097	5.007	-0.449
Türkiye	0.000	0.008		0.158
Uruguay	0.000	-0.003		0.140
United States	0.000	-0.001		0.176
Viet Nam	-0.101	-0.065	4.980	-0.524
South Africa	0.000	0.005		0.139
Rest of the world	0.000	0.003		0.221

Notes: The table reports percentage changes in welfare and CO₂ imports following the airspace closure. Results correspond to the baseline model with $\eta = 2.6$ and an air transport cost shock of $d_{ni}^{\text{air}} = 1.07$. The congestion specification uses $\lambda = (0.097, 0.07)$. Δ welfare is defined as the percentage difference in welfare changes between the model with substitution across transport modes and the Cobb–Douglas benchmark.

Table E.23: Welfare and Emissions Effects of Suez Canal Closure

Country	Welfare change	CO ₂ imports
Australia	-0.174	-1.892
Benin	-0.052	
Belize	0.186	
Brazil	0.013	1.478
Brunei Darussalam	0.199	1.286
Canada	-0.001	0.665
Chile	0.030	0.402
China	-0.206	-8.071
Côte d'Ivoire	0.112	6.197
Colombia	0.075	1.562
Costa Rica	0.106	
Dominican Republic	0.007	-0.541
Ecuador	0.104	0.809
Europe	-0.863	3.953
Indonesia	-0.478	-11.362
Jamaica	-0.016	-0.128
Japan	-0.115	-3.213
Madagascar	-1.260	-0.163
Mexico	0.124	1.081
Myanmar	-0.555	-8.929
Mauritius	-1.253	
Malaysia	-0.870	-8.598
Nigeria	0.063	5.750
Peru	0.060	1.544
Philippines	-0.314	-4.174
Singapore	-0.896	-3.940
Thailand	-0.789	-8.160
Türkiye	-1.121	5.403
Uruguay	0.034	1.110
United States	0.000	1.521
Viet Nam	-1.090	-13.241
South Africa	0.085	0.876
Rest of the world	0.059	2.799

Notes: The table reports percentage changes in welfare and CO₂ imports following the Suez Canal closure. Results correspond to the baseline model with $\eta = 2.6$ and the increase in maritime costs is based on the increase in distance from Feyrer (2019). The congestion specification uses $\lambda = (0.097, 0.07)$. Welfare changes are reported relative to the initial equilibrium.

Table E.24: Welfare and Emissions Effects of the IMO 2023 Policy

Country	Welfare change	Δ welfare	CO ₂ imports
Australia	-1.708	2.456	-13.749
Benin	-2.243	0.921	
Belize	-2.060	1.558	
Brazil	-0.941	1.235	-25.037
Brunei Darussalam	-2.670	1.236	-18.791
Canada	-1.422	1.317	-10.502
Chile	-1.160	1.329	-12.705
China	-2.538	2.321	-20.334
Côte d'Ivoire	-1.606	1.098	-32.368
Colombia	-1.493	1.215	-16.912
Costa Rica	-1.688	1.191	
Dominican Republic	-1.454	1.153	-1.740
Ecuador	-1.478	1.254	-13.541
Europe	-1.947	2.198	-12.533
Indonesia	-2.043	1.811	-16.768
Jamaica	-1.584	1.149	-4.230
Japan	-1.822	1.936	-14.417
Madagascar	-1.915	1.087	-11.120
Mexico	-1.321	1.219	-17.482
Myanmar	-2.261	1.833	-18.835
Mauritius	-1.886	1.121	
Malaysia	-2.160	1.986	-19.790
Nigeria	-1.554	1.085	-30.245
Peru	-1.361	1.257	-17.006
Philippines	-2.130	2.085	-21.593
Singapore	-2.452	1.734	-19.078
Thailand	-2.181	2.036	-20.602
Türkije	-1.731	1.292	-14.463
Uruguay	-1.284	1.238	-16.303
United States	-1.153	1.193	-18.552
Viet Nam	-2.210	2.017	-22.614
South Africa	-1.498	1.174	-15.904
Rest of the world	-1.579	1.223	-18.881

Notes: The table reports percentage changes in welfare and CO₂ imports under the IMO 2023 policy counterfactual. Results correspond to the baseline model with congestion, using $\lambda = (0.097, 0.07)$. Δ welfare is defined as the percentage difference in welfare changes between the model with substitution across transport modes and the Cobb–Douglas benchmark.